KERNFORSCHUNGSZENTRUM

KARLSRUHE

Mai 1975 KFK 2127

Institut für Angewandte Kernphysik

Empirical Studies of the Effective Interaction and of Exchange Effects for the Folding Model Approach of 104 MeV α-Particle Scattering

H.J. Gils, H. Rebel

GESELLSCHAFT
FÜR
KERNFORSCHUNG M.B.H.

KARLSRUHE

GESELLSCHAFT FÜR KERNFORSCHUNG M. B. H.

KARLSRUHE

KERNFORSCHUNGSZENTRUM KARLSRUHE

KFK 2127

Institut für Angewandte Kernphysik

Empirical Studies of the Effective Interaction and of Exchange Effects for the Folding Model Approach of 104 MeV α-Particle Scattering

H.J. Gils and H. Rebel

Gesellschaft für Kernforschung mbH, Karlsruhe

ABSTRACT

Differential cross sections of elastic 104 MeV α-particle scattering from several target nuclei between ^{12}C and ^{116}Sn have been analyzed by a semimicroscopic folding model in order to obtain an adequate normalization of the effective nucleon-α-interaction and to study the influence of the normalization on the extracted rms-radii of the nuclear matter. By additionally introducing an effective exchange potential we studied the dependence of the matter parameters on exchange effects. Furthermore the exchange potential was applied to the inelastic scattering from ^{20}Ne, ^{56}Fe, ^{58}Ni, ^{60}Ni, ^{90}Zr, and ^{116}Sn. No significant deviations between deformation parameters and rms-radii, respectively, extracted with and without exchange potential could be observed. Isocalar transition rates have been determined and have been compared to results from different methods.

Empirische Untersuchungen der effektiven Wechselwirkung und der Austauscheffekte in der Faltungsmodellnäherung für 104 MeV α-Teilchen Streuung.

ZUSAMMENFASSUNG

Differentielle Wirkungsquerschnitte der elastischen Streuung von 104 MeV α-Teilchen an verschiedenen Targetkernen zwischen ^{12}C und ^{116}Sn wurden im Rahmen eines halbmikroskopischen Faltungsmodells analysiert, um eine geeignete Normierung der effektiven Wechselwirkung zu gewinnen. Der Einfluß der Normierung auf extrahierte mittlere quadratische Radien der Nukleonendichteverteilung wurde untersucht. Durch Einführung eines zusätzlichen Austausch-Pseudopotentials studierten wir die Abhängigkeit der Parameter der Dichteverteilung von Austauscheffekten. Darüberhinaus wurde das Austauschpotential bei der Analyse der inelastischen Streuung von ^{20}Ne, ^{56}Fe ^{58}Ni, ^{60}Ni, ^{90}Zr und ^{116}Sn angewendet. Es wurden keine Unterschiede der Deformationsparameter und mittleren quadratischen Radien zwischen den Analysen mit oder ohne Austauschpotential beobachtet. Aus den Resultaten der Nukleonendichteverteilungen wurden isokalare Übergangswahrscheinlichkeiten berechnet und mit Ergebnissen anderer Methoden verglichen.

1. INTRODUCTION

To the lowest order of a multiple scattering expansion the real part $U_R(\vec{r}_\alpha)$ of the optical potential is generated by averaging an effective projectile-bound-nucleon interaction $V_{eff}(\vec{r}_\alpha,\vec{r})$ over the nucleon density distribution $\rho_m = \langle 0|\sum_i^A \delta(\vec{r}-\vec{r}_i)|0\rangle$ of the target:

$$U_R(\vec{r}_\alpha) = \int V_{eff}(\vec{r}_\alpha,\vec{r})\ \rho_m(\vec{r})\ d^3r \tag{1.1}$$

The folding model description of scattering of nuclear particles from nuclei is based on such a simple expression neglecting all higher order terms, the polarizibility of a complex projectile and effects arising from antisymmetrization and exchange between projectile and target. This approach has been extensively applied in recent α-particle scattering studies in order to extract nuclear size and shape information from measured differential scattering cross sections. As shown in a recent review |Re 74| this approach is very successful and resulted in values of the rms-radii and of the nuclear deformation completely in agreement with results from other methods. However, before unambiguous information concerning the nucleon density distribution ρ_m can be deduced by the folding procedure one has to determine the effective interaction and to reduce its uncertainties to a minimum. The effective α-particle nucleon interaction has been discussed frequently, |Gl Ve 66, Be 69, Ba Fr 71, Le Hi 72, Bu Du 70|. One approach |Gl Ve 66, Be 69, Bu Du 70| uses a double folding procedure and derives the α-nucleon interaction by averaging the nucleon-nucleon interaction over the internal motion of the α-particle. Batty et al. |Ba Fr 71| compared these attempts and concluded that the best choice for a local effective interaction is of the simple Gaussian form

$$V_{eff} = \lambda_R(E) \cdot V_0 \exp\left[-|\vec{r}-\vec{r}_\alpha|^2/\mu_0^2\right] \tag{1.2}$$

The strength V_0 and the range μ_0 were determined by Bernstein |Be 69| to be $V_0 = 37$ MeV and $\mu_0 = 2.0$ fm. As pointed out by Batty et al. |Ba Fr 71| these values have to be corrected since Bernsteins derivation used the rms-radius of the charge distribution instead of the nucleon matter radius of the α-particle. The corrected values are $V_0 = 43$ MeV and $\mu_0 = 1.901$ fm.

Zum Druck eingereicht am 24.3.1975

The energy dependent factor $\lambda_R(E)$ is a "renormalization" of the free α-nucleon interaction due to the influence of the other bound nucleons. It has been argued that the quantity λ_R can be determined by calibrating the effective interaction at the α-particle scattering from ^{40}Ca. The nucleus ^{40}Ca is the heaviest T=0 nucleus and no difference between proton and neutron distribution is expected so that ρ_m may be taken from electron scattering results. Following this proposal of Bernstein and Seidler |Be Se 71| Lerner et al. |Le Hi 72| investigated the elastic α-particle scattering from ^{40}Ca between 40 and 115 MeV projectile laboratory energy and deduced values and energy dependence of λ_R on the basis of a Gaussian interaction with μ_o = 2.0 fm (and V_o = 37 MeV).

In the present paper we report similar studies of a Gaussian effective interaction with the corrected value of the range parameter μ_o = 1.901 fm in order to provide a reliable value of λ_R for E_α = 104 MeV. Starting with nucleon density distributions the parameters of which are taken from electromagnetic results we extend previous investigations over ten nuclei from ^{12}C to ^{116}Sn aiming at some information about a possible A-dependence and specific nuclear structure effects of the λ_R value. Furthermore the influence of exchange effects on the results of the folding model procedure are studied. Exchange effects are often said to be important |Scha 70| , in particular for inelastic transitions of high multipolarities, and they may influence the values of the free parameters of the transition densities extracted by the analyses. In particular, exchange corrections may affect the values of the deformation parameters when in the framework of collective models the transition densities are derived from deformed distributions ρ_m. It is the purpose of this paper to explore these and other sensitivities on the parameters of the effective interaction and of the nuclear matter distributions, respectively.

The investigations are based on the data taken at E_α = 104 MeV and collected for several years by the group at the Karlsruhe Isochronous Cyclotron |Ha Lö 69 , Ha Ha 70 , Re Lö 72 a , Re Sc 72 b , Gi Re 74 a|. The differential cross sections are measured with high angular accuracy

and in sufficiently small angle steps so that position and slope of the diffraction oscillations are well determined. This is just the type of measured angular distributions which can reveal agreement and deficiencies of the reaction model under consideration. In most cases the Karlsruhe data are restricted to the forward region where the pronounced diffraction patterns are observed. We feel that such a restriction is in the spirit of the simple folding model represented by eq. 1.1 and based on "elementary" α-particles which interact only in the low density region of the nucleus. Certainly, the differential cross sections at backward angles reveal more complicated features of the reaction mechanism when the α-particles are probing deeper into the nucleus. But with the aspect of providing a tool for studies of the nuclear surface an application of the folding concept to the angular distributions of the backward angles would bring up more uncertainties rather than refined information on the nucleus.

2. STUDIES OF THE PARAMETER λ_R

2.1 General Procedure

We assume that for not too heavy nuclei the nucleon and the proton distribution are identical and introduce into eq. 1.1 a distribution ρ_m derived from experimental results of nuclear charge distributions by unfolding the charge distribution of a single proton via the relation

$$(2.1) \qquad \langle r^2 \rangle_{ch} = \langle r^2 \rangle_p + \langle r^2 \rangle_{s.p.} = \langle r^2 \rangle_m + \langle r^2 \rangle_{s.p.}$$

For the rms-radius $\langle r^2 \rangle_{s.p.}^{1/2}$ of a single proton the value of 0.8 fm is adopted. As functional form of the distribution a two-parameter Fermi distribution (w=o) or a parabolic Fermi distribution is used.

$$(2.2) \qquad \rho(r) = \rho_o \left[1 + \exp\left(\frac{r-c}{a}\right)\right]^{-1} \left(1+w\frac{r^2}{c^2}\right)$$

Converting charge distributions to nucleon distributions the difference $\langle r^2 \rangle_{ch} - \langle r^2 \rangle_m$ (eq. 2.1) is ascribed to a change of $c = c_{ch} \rightarrow c = c_m$ while the other parameters remain fixed. Preceeding studies| Ma Li 73, Gi Re 74 b| showed that the differential cross sections are less sensitive to the specific values of c_m and a_m provided that the combination reproduces the

correct value of the rms-radius. The values for the charge distributions are taken from a compilation of Hofstadter and Collard |Ho Co 67| who presented as empirical A-dependence of the rms-radii

$$\langle r^2 \rangle_{ch}^{1/2} = 0.82 \cdot A^{1/3} + 0.58 \quad [fm]$$

From the average value of the measured rms-radii quoted by Hofstadter and Collard c_m is deduced using the relations (2.1) and

$$c_m = \sqrt{\frac{5}{3} \langle r^2 \rangle_m - \frac{7}{3} \pi^2 a_m^2} \qquad \text{and}$$

assuming $a_m = 0.5$. According to Elton |El 61| the half-way radius c_{ch} of a two parameter Fermi distribution follows

$$c_{ch} = 1.115 \cdot A^{1/3} - 0.53 \cdot A^{-1/3} \quad [fm]$$

with $a_{ch} = 0.57$ fm for $A \geq 20$ while for ^{16}O and ^{12}C $a_{ch} = 0.46$ fm is recommended as a suitable value |c.f. El 61|. Since the choice of the rms-radius affects the results much more than the particular functional form of the distribution the effects of various values of the rms-radius (compiled in tab. 1 for convenience) are compared.

In our calculations the imaginary part $U_I(\vec{r}_\alpha)$ of the optical potential was treated in two different representations: the macroscopic three parameter Saxon-Woods form

$$U_I(\vec{r}_\alpha) = W_o \left[1 + \exp\left(\frac{\vec{r}_\alpha - R_w}{a_w}\right)\right]^{-1} \tag{2.3}$$

and alternatively, according to Bernstein's proposal |Be Se 71|

$$U_I(\vec{r}_\alpha) = (\lambda_I/\lambda_R) \cdot U_R(\vec{r}_\alpha) \tag{2.4}$$

the imaginary part proportional to U_R. The latter representation is chosen for a direct comparison with other investigations although the macroscopic Saxon-Woods-form frequently results in better fits to the experimental data. The fact that two completely different representations of the imaginary part lead to satisfactory and consistent results is also a consequence of the strong absorption emphasizing the surface region of the potentials.

Nuclide	Experimental charge rms-radii [Ho Co 67] [fm]	Average of experimental values		Empirical formula of Hofstadter and Collard		Empirical formula of Elton	
		charge [fm]	nucleon matter [fm]	charge [fm]	nucleon matter [fm]	charge [fm]	nucleon matter [fm]
^{12}C	2.53; 2.58; 2.41; 2.47; 2.42; 2.35	2.46	2.33	2.457	2.323	2.469	2.336
^{16}O	2.75; 2.71; 2.79	2.75	2.63	2.646	2.522	2.630	2.506
^{20}Ne	2.91; 3.00	2.96	2.85	2.806	2.689	3.047	2.940
^{24}Mg	2.98; 2.91	2.95	2.84	2.945	2.835	3.160	3.057
^{28}Si	3.04; 3.14	3.09	2.99	3.070	2.964	3.266	3.166
^{32}S	3.12; 3.33; 3.19	3.21	3.11	3.183	3.081	3.360	3.264
^{40}Ca	3.50; 3.41; 3.49*	3.47	3.38	3.384	3.288	3.536	3.445
^{56}Fe	3.85; 3.75; 3.74	3.78	3.69	3.717	3.630	3.834	3.749
^{90}Zr	4.27**	4.27	4.19	4.255	4.179	4.332	4.257
^{116}Sn	4.55; 4.50; 4.67	4.57	4.50	4.579	4.509	4.639	4.570

Tab. 1 Rms-radii of charge and nucleon density distributions adopted for the analyses.

* From Frosch et al. [Fr Ho 68]

** From Brissaud et al. [Br Bo 72]

2.2 λ_R-calibration by elastic scattering from ^{40}Ca

The study of Lerner et al. |Le Hi 72| is based on a parabolic Fermi charge distribution of ^{40}Ca obtained by Frosch et al. |Fr Ho 68| The parameter values used were c_{ch} = 3.676 fm, a_{ch} = 0.585 fm and w = - 0.1017 resulting in a rms charge radius $\langle r^2 \rangle_{ch}^{1/2}$ = 3.487 fm and a rms radius of the proton density distribution $\langle r^2 \rangle_p^{1/2}$ = 3.394 fm. Lerner et al. fitted the measured differential cross sections for elastic scattering from ^{40}Ca by varying λ_R and λ_I. From the data measured by the Karlsruhe group at E_α = 104 MeV they found

$$\lambda_R = 0.86 \qquad \lambda_I = 0.48$$

Proceeding as described in sect. 2.1 we repeated first the analysis for E_α = 104 MeV with V_o = 37 MeV and μ_o = 2 fm. The obtained values given in tab. 2 are slightly different from the values of Lerner et al. This may be due to a different angular range used in the analysis and due to little differences in the procedure. Starting with the corrected range parameter μ_o = 1.901 fm an increased value of $\lambda_R \cdot V_o$ is expected according to the parameter ambiguity of the Gaussian interaction detected by Batty et al.| Ba Fr 71|

$$\lambda_R \cdot V_o \cdot \mu_o^6 = \text{const.}$$

The result given in tab. 2 is roughly in agreement with this relation. The values of the constant are 2060 MeV fm^6 and 1910 MeV fm^6, respectively.

Tab. 2 compiles the results of various analyses with different conditions. Some cases are displayed in fig. 1. For the angular range $\Theta \leq 40^o$ no significant difference of the extracted λ_R-values has been found for the two different representations of the imaginary potential. But there is also some indication that for the larger angular range including clearly damped oscillations the macroscopic imaginary potential requires a somewhat higher λ_R-value as Bernstein's representation. This may reflect that in general, λ_R is not independent of the geometry of the imaginary part.

λ_R	$c_m \cdot A^{-1/3}$ [fm]	a_m [fm]	w	$\langle r^2 \rangle_m^{1/2}$ [fm]	λ_I or W_o [MeV]*	r_w [fm]	a_w [fm]	V_o [MeV]	μ_o [fm]	Data range CM	χ^2/F
0.87(4)	1.032	0.5851	-0.1017	3.394	0.40(2)	-	-	37.	2.	< 75°	95.1
0.94(4)					0.44(2)			43.	1.901		77.5
0.95(4)	1.023	0.55	0.0	3.394	0.44(2)						75.1
0.99(2)					0.53(1)					< 40°	12.7
1.04(1)					31.(2)*	1.37(4)	0.91(5)			< 75°	55.4
0.978(2)					19.4(3)*	1.66(5)	0.57(7)			< 40°	1.1
0.96(3)	1.064	0.50		3.38	0.45(2)	-	-			< 75°	68.8
0.91(4)	1.027	0.57		3.444	0.42(2)						82.9
1.05(3)	1.024	0.50		3.288	0.50(2)						34.0
1.053(9)	1.22(2)	0.18(6)		3.30(4)	27.2(9)*	1.43(2)	0.84(4)				22.5
0.981(2)	1.034(8)	0.54(1)		3.39(4)	19.6(3)*	1.659(9)	0.58(1)			< 40	1.1

Tab. 2 Results of the analysis of elastic scattering from ^{40}Ca. For better reading of the table there is only a number or sign given when the value has changed compared to the line above. The numbers in brackets are the errors in the last digit. The definitions of the errors are given in [Re Sc 72b]. Parameters without an error given have been fixed.

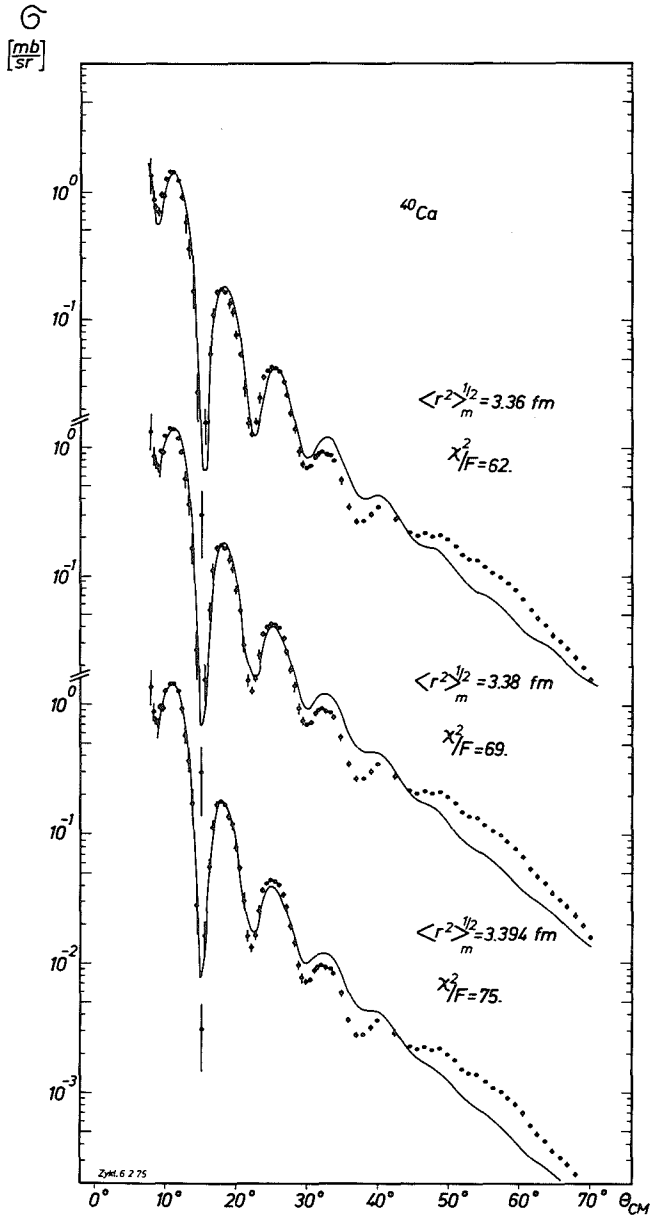

Fig. 1 Elastic differential cross sections of ^{40}Ca. For the calculated cross sections different rms radii of the nucleon distribution have been adopted.

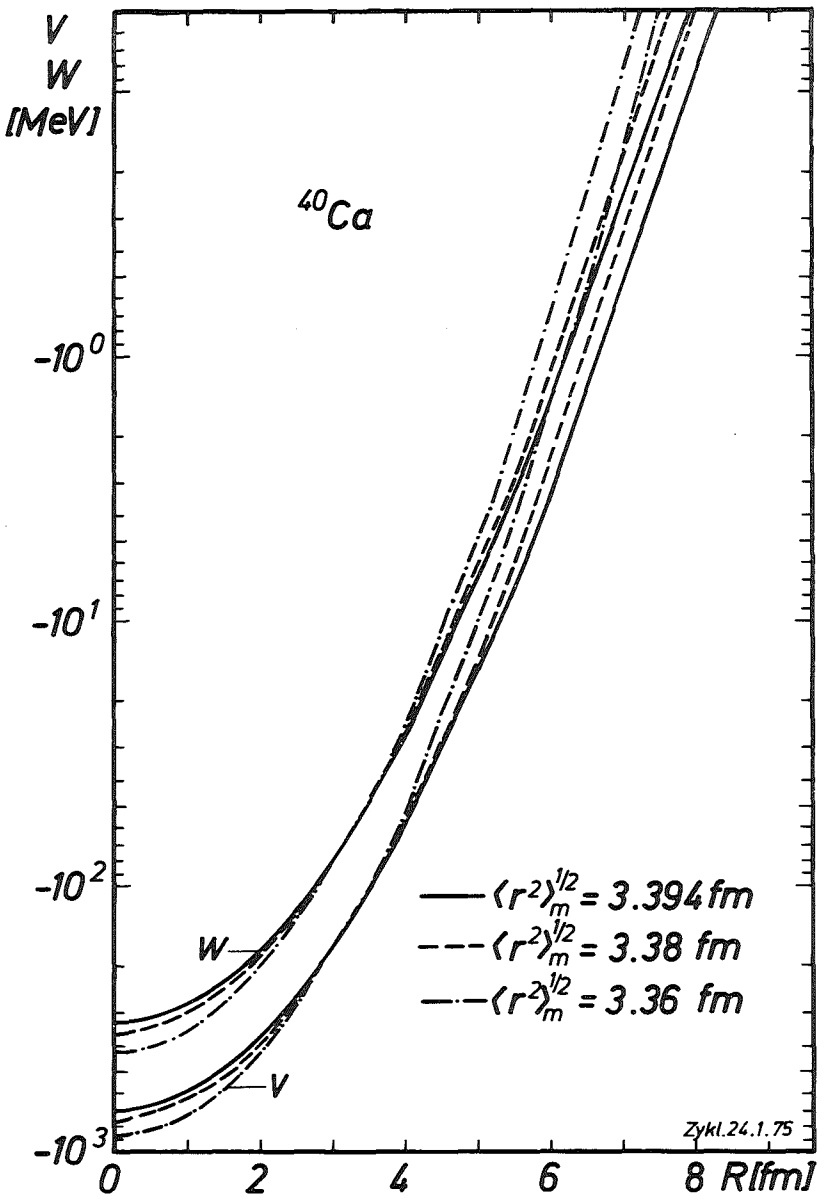

Fig. 2 Real (V) and imaginary(W) potentials of ^{40}Ca corresponding to the cross sections shown in fig. 1.

In particular, the extracted λ_R-values depend on the adopted rms-radius of ^{40}Ca. The values of λ_R and λ_I seem to decrease with increasing rms-radius. In all cases the corresponding real potentials show a similar radial behaviour in therange between 3.0 and 4.0 fm which is the sensitive region of the cross sections. Fitting the experimental data the potential parameters are adjusted in such a way that a certain radial behaviour is reproduced (see fig. 2). Assuming that the averaged value of the experimental rms-radii of 3.38 fm is the correct value it is seen that this value also results from the best fits to the data, and that fits resulting in less reasonable parameter values do reproduce the data with minor quality. Therefore, done with some caution, it may not be unreasonable to adjust λ_R in every specific case by a best fit and simultaneously extract correct information on ρ_m although λ_R is determined from an independent calibration only within a 10 percent limit and will vary in this limit dependent on the specific conditions.

2.3 A-dependence

The same procedure used in the case of ^{40}Ca is applied to the elastic scattering cross sections of ^{12}C, ^{16}O, ^{20}Ne, ^{24}Mg, ^{28}Si, ^{32}S, ^{56}Fe, ^{90}Zr and ^{116}Sn. Two parameter-Fermi distributions ρ_m which are consistent with averaged experimental rms-radii or with calculated values (see tab. 1) are introduced into the folding formula (eq. 1.1). The parameters λ_R and λ_I are varied. Results are given in tab. 3 a and 3 b. There is a significant variation of λ_R and λ_I with A reflecting a dependence of λ_R on the CM-energy |Le Hi 72| superimposed by fluctuations which may be due to some structure effects.+) Furthermore we see for light nuclei a difference in the λ_R-values extracted only from the region $\Theta_{CM} \leq 40^o$ or including larger scattering

+) The case of ^{24}Mg resulted in a relatively bad reproduction of the experimental data and deviations from the general trends. The origin of the behaviour is not understood (see also tab. 4).

Nuclide	Experimental rms-radii			Calculated rms-radii (Hofstadter/Collard)			Calculated rms-radii (Elton)			Average values		E_{CM}
	λ_R	λ_I	χ^2/F	λ_R	λ_I	χ^2/F	λ_R	λ_I	χ^2/F	λ_R	λ_I	[MeV]
^{12}C	0.75(2)	0.32(2)	49.3	0.75(2)	0.32(2)	50.0	0.75(2)	0.31(1)	42.0	0.75(1)	0.31(1)	78.
^{16}O	0.81(3)	0.34(2)	93.2	1.04(7)	0.46(4)	115.	1.06(7)	0.48(4)	118.	0.87(3)	0.38(2)	83.2
^{20}Ne	0.95(3)	0.51(2)	83.8	1.13(4)	0.60(3)	82.6	0.87(3)	0.45(2)	84.9	0.96(2)	0.50(1)	86.7
^{24}Mg	0.81(2)	0.54(1)	703.	0.81(2)	0.54(1)	701.	0.75(3)	0.50(2)	754.	0.80(1)	0.536(8)	89.1
^{28}Si	0.97(2)	0.48(1)	6.2	0.99(2)	0.49(1)	5.9	0.81(2)	0.41(2)	16.0	0.92(1)	0.477(8)	91.
^{32}S	-	-	-	-	-	-	-	-	-	-	-	92.4
^{40}Ca	0.96(3)	0.45(2)	68.8	1.05(3)	0.50(2)	63.2	0.91(4)	0.42(2)	82.9	0.98(2)	0.46(1)	94.5
^{56}Fe	0.92(1)	0.533(8)	16.6	0.99(1)	0.574(9)	17.1	0.86(1)	0.478(8)	19.1	0.923(6)	0.525(5)	97.1
^{90}Zr	0.99(2)	0.58(1)	66.7	1.00(2)	0.59(1)	67.1	0.95(2)	0.53(2)	63.	0.98(1)	0.58(1)	99.6
^{116}Sn	1.04(1)	0.70(1)	27.9	1.03(1)	0.69(1)	27.3	0.985(8)	0.631(8)	11.7	1.013(5)	0.667(5)	100.5

Tab. 3a

Nuclide	Experimental rms-radii			Calculated rms-radii (Hofstadter/Collard)			Calculated rms-radii (Elton)			Average values		E_{CM}
	λ_R	λ_I	χ^2/F	λ_R	λ_I	χ^2/F	λ_R	λ_I	χ^2/F	λ_R	λ_I	[MeV]
^{12}C	1.09(4)	0.41(2)	14.3	1.09(4)	0.41(2)	14.2	1.078(6)	0.414(6)	8.2	1.08(2)	0.41(1)	78.
^{16}O	0.92(6)	0.42(3)	93.5	1.06(6)	0.46(4)	86.4	1.07(6)	0.46(4)	88.2	1.02(4)	0.44(2)	83.2
^{20}Ne	1.01(3)	0.59(3)	79.1	1.20(4)	0.69(3)	80.2	0.93(3)	0.53(2)	75.8	1.02(2)	0.58(2)	86.7
^{24}Mg	0.79(2)	0.54(1)	763.	0.79(2)	0.55(1)	763.	0.72(2)	0.49(2)	708.	0.77(1)	0.539(8)	89.1
^{28}Si	0.97(1)	0.502(9)	2.9	1.00(1)	0.514(9)	2.7	0.81(2)	0.43(2)	11.0	0.966(8)	0.501(8)	91.
^{32}S	1.00(2)	0.55(2)	22.9	1.03(2)	0.57(7)	23.6	0.86(2)	0.46(1)	16.4	0.96(1)	0.48(2)	92.4
^{40}Ca	1.01(2)	0.55(1)	11.4	1.11(2)	0.61(2)	12.1	0.94(2)	0.50(1)	14.2	1.02(1)	0.534(8)	94.5
^{56}Fe	0.930(9)	0.528(7)	12.7	1.00(1)	0.566(8)	13.5	0.867(9)	0.472(7)	15.3	0.928(5)	0.518(4)	97.1
^{90}Zr	0.98(1)	0.541(9)	21.7	1.00(1)	0.55(1)	25.8	0.95(1)	0.50(1)	19.9	0.977(6)	0.531(6)	99.6
^{116}Sn	1.03(1)	0.70(2)	31.8	1.03(1)	0.69(2)	31.0	0.982(7)	0.633(8)	7.4	1.006(5)	0.65(1)	100.5

Tab. 3b

Tab. 3: Determination of λ_R and λ_I by fitting elastic α-particle differential cross sections based on fixed nucleon density distribution parameters. The radius parameters are deduced from tab. 1. The diffuseness adopted is 0.50 fm for columns 2 to 7 and 0.57 fm (^{12}C, ^{16}O:0.46) for columns 8 to 10. For details please refer to the text.

a) Data range $\theta_{CM} < 75^\circ$

b) Data range $\theta_{CM} < 40^\circ$

Nuclide	$c_m \cdot A^{-1/3}$ [fm]	a_m [fm]	λ_I	χ^2/F	$\langle r^2 \rangle_m^{1/2}$ [fm]	$\langle r^2 \rangle_{ch}^{1/2}$ [fm]
^{12}C	1.29(12)	0.33(10)	0.43(1)	34.9	2.60(18)	2.72
^{16}O	1.16(11)	0.38(8)	0.43(2)	106.3	2.67(16)	2.79
^{20}Ne	0.87(9)	0.58(4)	0.49(1)	82.4	2.84(12)	2.95
^{24}Mg	0.56(9)	0.66(3)	0.62(1)	585.	2.74(10)	2.85
^{28}Si	1.06(2)	0.44(2)	0.484(6)	5.5	2.98(4)	3.09
^{32}S	-	-	-	-	-	-
^{40}Ca	1.129(8)	0.41(2)	0.465(8)	62.0	3.36(3)	3.45
^{56}Fe	1.05(1)	0.52(2)	0.525(6)	20.5	3.66(4)	3.75
^{90}Zr	1.06(1)	0.56(2)	0.545(9)	63.5	4.24(4)	4.32
^{116}Sn	1.073(4)	0.590(8)	0.604(6)	10.8	4.61(1)	4.68

Tab. 4a

Nuclide	$c_m \cdot A^{-1/3}$ [fm]	a_m [fm]	λ_I	χ^2/F	$\langle r^2 \rangle_m^{1/2}$ [fm]	$\langle r^2 \rangle_{ch}^{1/2}$ [fm]
^{12}C	1.342(5)	0.11(4)	0.38(2)	9.0	2.50(3)	2.62
^{16}O	0.86(2)	0.52(7)	0.42(2)	94.7	2.57(19)	2.69
^{20}Ne	0.85(9)	0.60(4)	0.50(2)	86.7	2.85(12)	2.96
^{24}Mg	0.45(37)	0.70(6)	0.63(1)	599.	2.79(23)	2.90
^{28}Si	1.04(2)	0.47(1)	0.495(5)	2.2	2.99(3)	3.10
^{32}S	0.90(3)	0.61(2)	0.499(8)	15.9	3.16(6)	3.25
^{40}Ca	1.10(2)	0.49(2)	0.530(8)	11.4	3.43(4)	3.52
^{56}Fe	1.04(1)	0.52(1)	0.538(6)	12.6	3.66(2)	3.75
^{90}Zr	1.061(9)	0.56(1)	0.511(7)	20.1	4.24(3)	4.32
^{116}Sn	1.071(3)	0.597(6)	0.603(6)	5.1	4.62(1)	4.69

Tab. 4b

Tab. 4 Determination of the parameters of the nuclear matter distributions using $\lambda_F = 0.96$. Numbers in brackets are the errors in the last digits.

a) Data range $\theta_{CM} < 75^\circ$

b) Data range $\theta_{CM} < 40^\circ$

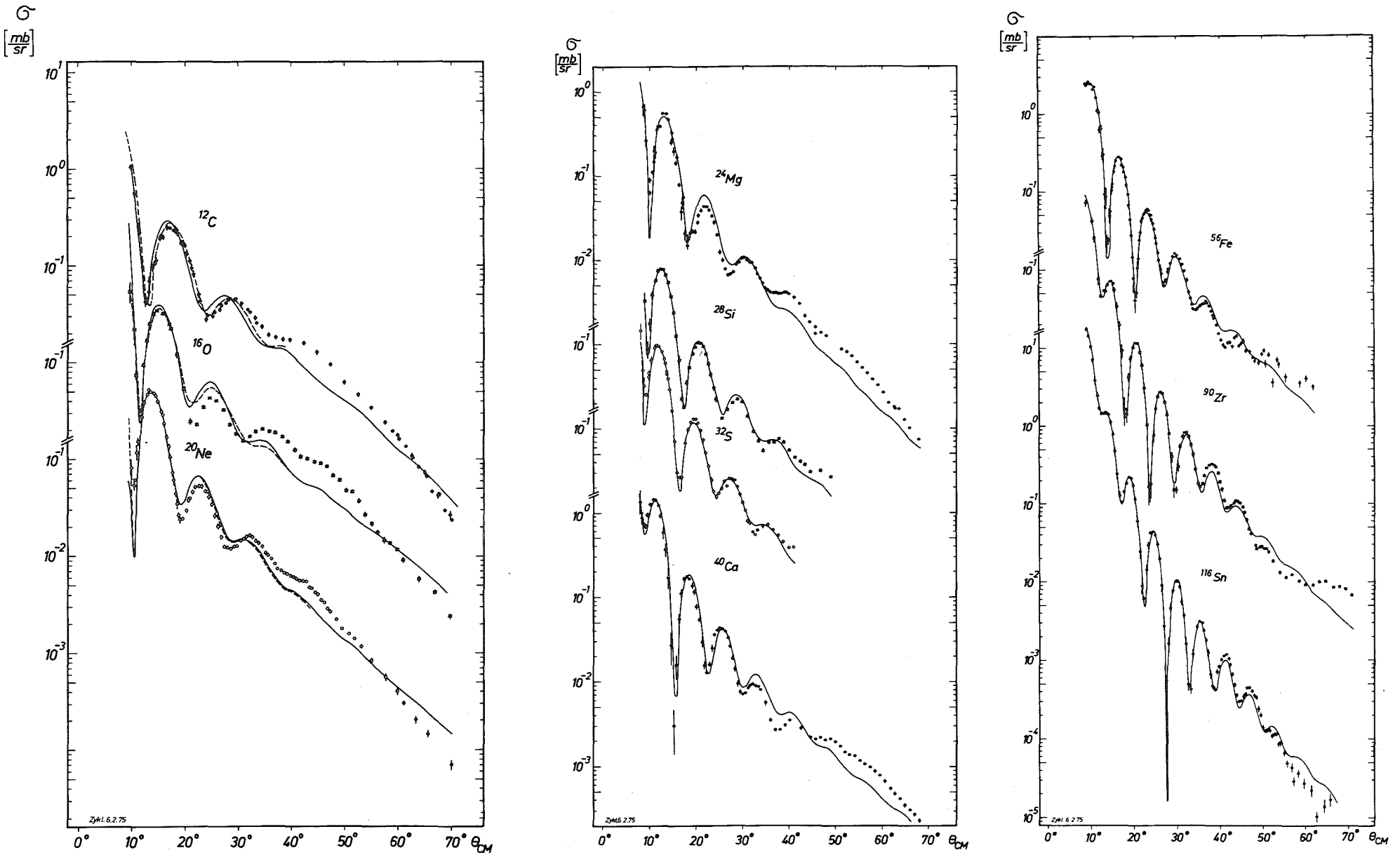

Fig. 3 Measured and calculated elastic differential cross sections using $\lambda_R = 0.96$. The dashed lines show the fit to data ranging only up to $\theta_{CM} \leq 40^\circ$

angles beyond the grazing collision region. Moreover in the case of ^{12}C the α-particles penetrate more deeply into the nucleus where the density distribution deviates from the Fermi shape. As compared to the uncertainties the energy variation of λ_R for the fixed laboratory energy of 104 MeV is not so pronounced we deduce from the results a weightened value $\overline{\lambda_R}=0.96 \pm 0.01$ which may serve as a first prediction and starting point for an analysis in a specific case. Inverting the procedure and using this λ_R-value fixed the parameters of the nucleon distribution are determined by fitting the differential cross sections and varying c_m, a_m and λ_I.

The resulting rms-radii (cf. tab. 4) are in good agreement with the electromagnetic results (cf. tab. 1). Only in the case of ^{12}C a larger discrepancy (cf. last column of tab. 4) is found which is reduced, when using only the forward scattering angles up to $\Theta_{cm} \leq 40^o$. The measured and calculated differential cross sections are shown in fig. 3. The quoted errors do not include systematical errors arising from the limits of the model |cf. Re Sc 72 b |.In order to get a feeling of the uncertainty due to the λ_R-value chosen the analysis is repeated by scanning the λ_R-value from 0.75 to 1.15 for the cases of ^{20}Ne and ^{56}Fe. This is demonstrated in tab. 5 a and 5 b. For ^{56}Fe the macroscopic representation of the imaginary potential is used.+)From the results we can deduce that an uncertainty $\Delta\lambda_R=0.1$ contributes to $\Delta\langle r^2\rangle_m^{1/2}$ by an additional uncertainty of about 2 %.

3. EXCHANGE EFFECTS

Effects arising from antisymmetrization and from exchange between projectile and target nucleons are not explicitely considered in the derivation of the effective interaction. Estimates of the importance of exchange effects can be made by use of a method proposed by Schaeffer |Scha 70| for DWBA analyses. Following this method we have to add a Gaussian pseudo potential

+) In this case the average value of λ_R obtained by the procedure described above proves to be $\lambda_R = 1.03$.

λ_R	$c_m \cdot A^{-1/3}$ [fm]	a_m [fm]	λ_I	χ^2/F	Data range	$\langle r^2\rangle_m^{1/2}$ [fm]	$\langle r^2\rangle_{ch}^{1/2}$ [fm]
0.75	1.29(4)	0.24(5)	0.402(7)	81.2	75°	2.86(7)	2.97
0.85	1.07(7)	0.49(4)	0.44(1)	85.2		2.90(11)	3.01
0.95	0.86(9)	0.59(4)	0.49(1)	82.8		2.85(12)	2.96
1.05	0.8 (1)	0.61(4)	0.54(1)	80.0		2.77(12)	2.88
1.15	0.7 (1)	0.61(4)	0.59(2)	78.5		2.70(5.10)	2.81
0.75	1.07(7)	0.58(4)	0.41(1)	82.5	40°	3.12(11)	3.22
0.85	0.96(8)	0.60(4)	0.47(2)	78.9		3.01(12)	3.11
0.95	0.8 (1)	0.63(4)	0.52(2)	74.0		2.90(12)	3.01
1.05	0.7 (1)	0.64(3)	0.57(2)	71.1		2.81(11)	2.92
1.15	0.6 (2)	0.65(4)	0.62(2)	70.0		2.72(15)	2.84
0.96	0.87(9)	0.58(4)	0.49(1)	82.4	75°	2.84(12)	2.95

Tab. 5a

λ_R	$c_m \cdot A^{-1/3}$ [fm]	a_m [fm]	W_o [MeV]	r_w [fm]	a_w [fm]	χ^2/F	Data range	$\langle r^2\rangle_m^{1/2}$ [fm]	$\langle r^2\rangle_{ch}^{1/2}$ [fm]
0.75	1.17(1)	0.51(2)	22.8(8)	1.61(1)	0.53(1)	8.8	75°	3.95(3)	4.03
0.85	1.12(2)	0.54(3)	38.(2)	1.54(2)	0.51(3)	15.1		3.88(6)	3.96
0.95	1.05(2)	0.56(2)	30.(2)	1.57(2)	0.53(2)	13.3		3.74(5)	3.83
1.05	1.06(5)	0.52(4)	67.(10)	1.45(5)	0.52(3)	14.5		3.70(9)	3.79
1.15	1.00(6)	0.56(4)	62.(31)	1.46(6)	0.53(3)	14.6		3.60(9)	3.69
0.75	1.17(1)	0.52(2)	25.(2)	1.59(1)	0.54(2)	7.5	40°	3.95(4)	4.03
0.85	1.06(2)	0.54(3)	21.(1)	1.55(3)	0.65(3)	9.6		3.73(6)	3.82
0.95	1.07(4)	0.54(3)	38.(9)	1.53(3)	0.52(2)	10.4		3.76(7)	3.85
1.05	0.97(1)	0.57(2)	21.8(6)	1.57(2)	0.61(3)	5.4		3.56(4)	3.65
1.15	1.01(6)	0.55(4)	68.(40)	1.44(6)	0.52(3)	11.2		3.62(9)	3.70
1.03	1.07(5)	0.52(4)	62.(27)	1.46(5)	0.52(3)	14.5	75°	3.71(9)	3.80

Tab. 5b

Tab. 5 Dependence of the nuclear matter distribution parameters on λ_R obtained from fits to elastic scattering cross sections.

a) ^{20}Ne

b) ^{56}Fe

(3.1) $$V_E = V_o^E(E_\alpha)\ \exp(-|\vec{r}-\vec{r}_\alpha|^2/\mu_E^2)$$

to the direct term $V^D(\vec{r}) \equiv V_{eff}(\vec{r})$ (eq. 1.2). Assuming a Gaussian nucleon-nucleon interaction $v = V_n e^{-(r/\mu_n)^2}$, according to Schaeffer|Scha 70| the effective interaction including exchange effects can be written

(3.2) $$V^{D+E} = V_o^D\ (\frac{\mu_n}{\mu_D})^3\ \exp(-|\vec{r}-\vec{r}_\alpha|^2/\mu_D^2)$$
$$+ V_o^E\ \exp(-\frac{1}{4}\,k^2\mu_n^2)(\frac{\mu_n}{\mu_E})^3 \exp(-|\vec{r}-\vec{r}_\alpha|^2/\mu_E^2)$$

with $k = \frac{m_n}{m_\alpha}\sqrt{2\cdot m_\alpha \cdot E} = \frac{1}{4}\,k_\alpha$ (wave number of the incident nucleon with the same energy as the composite α-particle). The range parameters μ_n, μ_D and μ_E are related by

$$\mu_D^2 = \mu_n^2 + \mu_E^2$$

We adopt for μ_n the value of 1.52 fm |Sa 71, Be 69| and for μ_E the value of 1.31 fm |Schae 70| resulting in μ_D = 2.01 fm. Furthermore a Serber exchange mixture $V_o^E / V_o^D = 1$|Ba Fr 71, Re Ta 70, Schae 70|is assumed. From this and taking $V_o = V_o^D\ (\frac{\mu_n}{\mu_D})^3$ = 43 MeV we replace the effective interaction of eq. 1.2 by

(3.3) $$V_{eff}^{D+E} = \lambda_R^{D+E} \cdot \{43\cdot\exp(-|\vec{r}-\vec{r}_\alpha|^2/(2.01)^2)$$
$$+\ 75\ \exp(-|\vec{r}-\vec{r}_\alpha|^2/(1.31)^2)\}$$

for E_α = 104 MeV.

The inclusion of an explicit exchange term in V_{eff} requires a readjustment of the λ_R-value in order to reproduce the experimental cross sections. Fig. 4 displays for ^{40}Ca the real potential $U_R \equiv V$ corresponding to eq. 3.3 (λ_R^{D+E}=0.62) and compares it to the results neglecting exchange (eq. 1.1 λ_R = 0.96 with μ_o = 1.901).

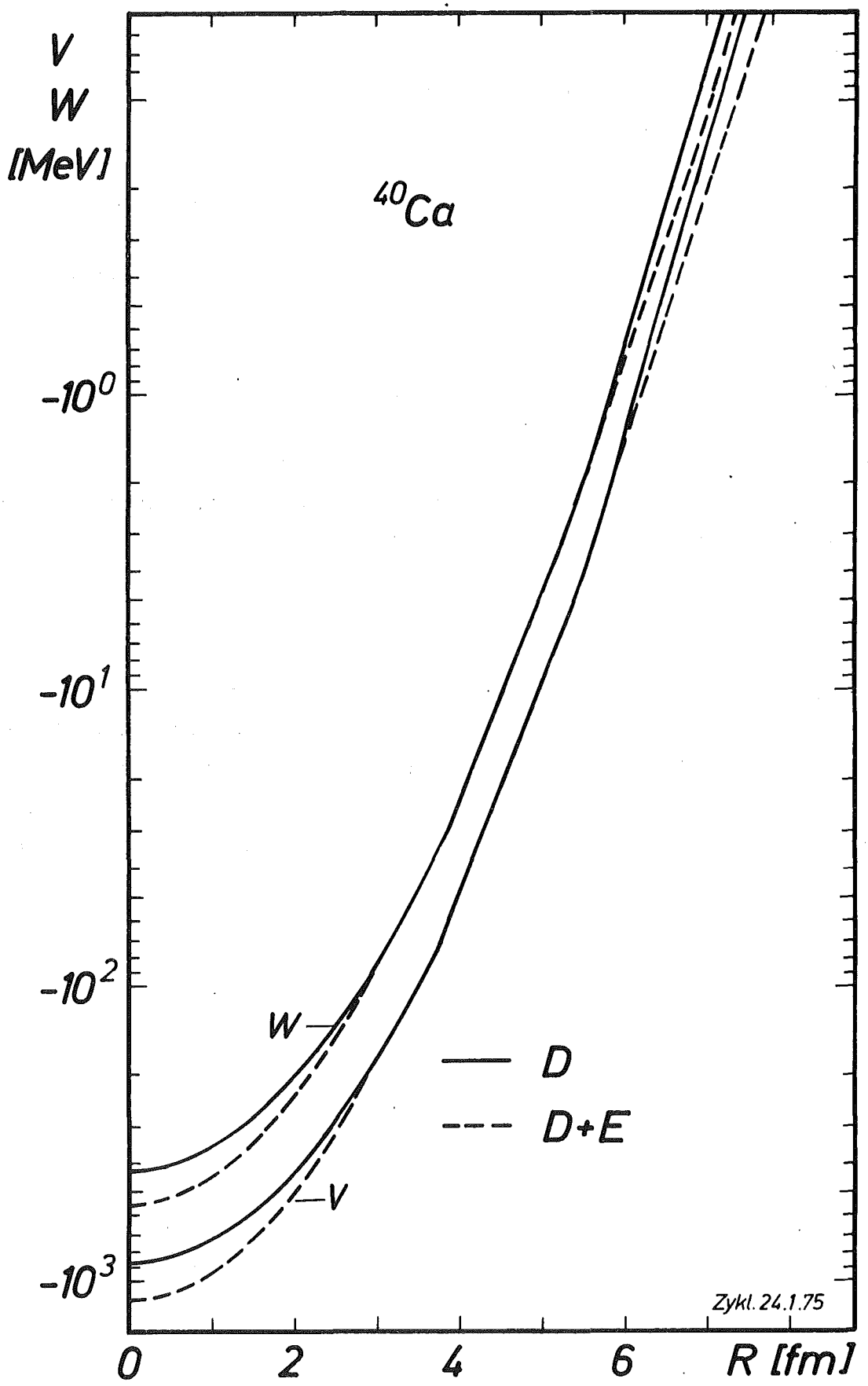

Fig. 4 Real (V) and imaginary(W) potentials of ^{40}Ca without (D; λ_R = 0.96) and with (D + E; λ_R = 0.62) exchange term. The corresponding nucleon density parameters are given in tab. 4 and tab. 6, respectively.

We see that the exchange term leads to a steeper slope (smaller diffuseness) which can be roughly compensated in the surface region by a larger value of λ_R when neglecting the exchange term.

Proceeding as in sect. 2.3 an average value $\overline{\lambda_R^{D+E}} = 0.62$ is deduced by fitting the data on the basis of eq. 3.3. The particular values for the nuclei fluctuate around this value qualitatively in the same manner as previously the results in tab. 3.

A compilation of elastic scattering analyses including the exchange potential and using $\lambda_R = 0.62$ fixed is given in tab. 6. There is nearly no difference between the matter parameters obtained with and without exchange potential (compare tab. 6 and tab. 4). The calculated cross sections do not deviate from those shown in fig. 3.

4. INELASTIC SCATTERING

The natural extension of the folding approach to inelastic scattering from collective states is introducing adequately deformed density distributions $\rho_m(\vec{r})$ into eq. 1.1. For this we use as standard prescription (which is certainly not the most general way of deforming a nucleus |Tas 73|) an angular dependence of the half-way radius c_m of the two-parameter Fermi form. For a permanent deformation we refer to a body fixed system.

$$(4.1) \qquad c_m(\Omega') = c_o(1 + \sum_{L,M} \beta_{LM} Y_{LM}(\Omega'))$$

If we assume axial symmetry terms with $M \neq 0$ vanish. More generally in the space fixed system c_m is parametrized by

$$(4.2) \qquad c_m(\Omega) = c_o(1 + \sum_{L,M} \alpha_{LM} Y_{LM}(\Omega))$$

including dynamic deformation (vibrations). The interesting quantities are the deformation parameters β_{LM} and matrix elements of the transition operators which are built up by the operators α_{LM}.

Nuclide	$c_m \cdot A^{-1/3}$ [fm]	a_m [fm]	λ_I	χ^2/F	$\langle r^2 \rangle_m^{1/2}$ [fm]	$\langle r^2 \rangle_{ch}^{1/2}$ [fm]
^{12}C	1.23(21)	0.41(13)	0.30(1)	61.8	2.67(25)	2.78
^{16}O	0.83(20)	0.54(7)	0.27(1)	118.4	2.59(23)	2.71
^{20}Ne	0.90(8)	0.57(3)	0.319(7)	78.5	2.85(9)	2.96
^{24}Mg	0.56(8)	0.65(2)	0.392(7)	569.	2.70(7)	2.82
^{28}Si	1.09(7)	0.42(2)	0.303(4)	4.9	3.00(6)	3.10
^{32}S	0.89(4)	0.60(2)	0.319(5)	15.7	3.13(6)	3.23
^{40}Ca	1.13(1)	0.42(2)	0.294(4)	58.2	3.38(4)	3.47
^{56}Fe	1.05(1)	0.51(1)	0.351(4)	17.1	3.65(2)	3.74
^{90}Zr	1.07(1)	0.54(2)	0.352(6)	64.0	4.22(4)	4.30
^{116}Sn	1.070(5)	0.586(9)	0.391(4)	11.2	4.59(2)	4.66

Tab. 6 Results of elastic scattering analyses including exchange effects ($\lambda_R = 0.62$). The numbers in brackets indicate the errors in the last digits.

The derivation of the form factors for DWBA or CC calculations is straight forward and given in detail in ref. |Re 74|. As due to the strong coupling higher order excitation processes affect the cross sections and provide additional information we use the coupled channel method for calculating the differential cross sections. The numerical calculations were carried out with the modified Karlsruhe version |Sc Ra 73| of the ECIS code. In general terms up to L = 4 are considered in eq. (4.1) and (4.2). Coulomb excitation is included by using a deformed Coulomb potential. Using the two alternative ways (eq. 2.3 and 2.4) in treating the imaginary potential we introduce a complex coupling.
In the case of the Saxon-Woods representation of the imaginary part the deformation of the imaginary potential is taken from preceding calculations on the basis of the extended optical potential.

The main purpose of the inelastic scattering analyses is a study of the applicability of the effective interaction derived from elastic scattering and of the influence of the exchange on the extracted nucleon density parameters, in particular, on the values of the deformation parameters. These questions are studied in six cases on the basis of several collective descriptions: ^{20}Ne, ^{56}Fe (symmetric rotator), ^{58}Ni, ^{60}Ni (anharmonic vibrator |Ta 65, 66, Re Lö 72 a|) ^{90}Zr, ^{116}Sn (harmonic quadrupole-octupole vibrator). We compare results of analyses (adjusting radius, diffusseness and deformation parameters of the nucleon density distributions) with (E) and without exchange pseudo potential using the corresponding expressions for the effective interactions (eq. 1.2 and 3.3, respectively), and $\overline{\lambda_R}$-values. The results are compiled in tab. 7 and displayed in fig. 5 a - c. When introducing the exchange potential the values of the diffuseness parameters are slightly decreased in favor of a slight increase of the radius c_m. Within the error bars the values of the deformation parameters remain unchanged, even for the transition multipolarity L = 4. This shows that for E_α = 104 MeV the exchange contribution is completely absorbed in the phenomenologically adjusted λ_R-value of eq. 1.2. The influence of a significant mismatch of λ_R is demonstrated in the cases of ^{56}Fe and ^{116}Sn using for V_{eff} the expression with exchange potential (eq.3.3) but with the λ_R-value of 0.96) as for eq. 1.2). This requires smaller c_m, larger a_m and β_L-values in order to

Nuclide	λ_R	λ_I or W_o[MeV]*	$c_m \cdot A^{-1/3}$ [fm]	a_m [fm]	β_2	β_4	$\langle r^2 \rangle_m^{1/2}$ [fm]	χ^2/F	Procedure
^{20}Ne	0.96	0.348(4)	1.09(1)	0.42(4)	0.436(7)	0.29(1)	2.94(8)	40.8	A, dC
	0.62	0.215(3)	1.12(6)	0.40(5)	0.41(2)	0.28(2)	2.95(15)	46.2	A, dC, E
^{56}Fe	0.96	0.461(4)	1.11(1)	0.46(2)	0.228(4)	0.037(7)	3.75(4)	19.2	A, dC
	1.03	25.(2)*	1.12(2)	0.47(2)	0.226(5)	0.009(7)	3.79(6)	16.4	A, dC, MI
	0.62	0.292(3)	1.13(2)	0.43(2)	0.222(4)	0.035(6)	3.75(6)	20.5	A, dC, E
	0.67	21.(1)*	1.021(3)	0.556(5)	0.240(4)	0.028(4)	3.70(1)	15.5	A, dC, E, MI
	0.96	0.436(4)	0.91(1)	0.52(1)	0.277(6)	0.046(8)	3.36(3)	21.1	A, dC, E

Nuclide	λ_R	λ_I or W_o[MeV]*	$c_m \cdot A^{-1/3}$ [fm]	a_m [fm]	β_{02}	β_{04}	β_{24}	$\langle r^2 \rangle_m^{1/2}$ [fm]	χ^2/F	Procedure
^{58}Ni	0.96	0.473(5)	1.09(1)	0.48(2)	0.157(5)	0.121(4)	0.08	3.73(5)	23.4	B, dC
	0.62	0.300(3)	1.10(2)	0.48(2)	0.153(6)	0.115(4)	0.08	3.74(5)	23.9	B, dC, E
^{60}Ni	0.96	0.478(5)	1.09(1)	0.48(1)	0.184(5)	0.108(5)	0.08	3.75(4)	14.4	B, dC
	0.62	0.302(3)	1.11(1)	0.46(2)	0.175(6)	0.107(5)	0.08	3.76(4)	14.2	B, dC, E

Nuclide	λ_R	λ_I or W_o[MeV]*	$c_m \cdot A^{-1/3}$ [fm]	a_m [fm]	β_2	β_3	$\langle r^2 \rangle_m^{1/2}$ [fm]	χ^2/F	Procedure
^{90}Zr	0.96	0.499(4)	1.098(9)	0.49(2)	0.075(2)	0.170(2)	4.22(4)	27.0	C
	0.96	0.498(4)	1.089(9)	0.51(1)	0.081(2)	0.179(3)	4.23(3)	26.5	C, dC
	0.62	0.319(3)	1.10(1)	0.49(2)	0.080(2)	0.177(3)	4.23(4)	26.0	C, dC, E
^{116}Sn	0.96	0.540(3)	1.125(4)	0.502(7)	0.112(1)	0.154(2)	4.64(2)	11.9	C
	0.96	0.540(4)	1.119(4)	0.513(8)	0.123(2)	0.162(2)	4.64(2)	10.5	C, dC
	0.62	0.348(3)	1.129(5)	0.497(9)	0.122(2)	0.161(2)	4.65(2)	10.6	C, dC, E
	0.96	0.529(4)	0.977(1)	0.568(3)	0.144(2)	0.192(2)	4.25(1)	10.7	C, dC, E
	0.62	0.348	1.125	0.502	0.112	0.154	4.64	12.8	C, E

Tab. 7 Inelastic scattering analyses without and with exchange term (E). The collective models used are: A: symmetric rotator model; B: Tamura's [Ta 72] anharmonic vibrator model; C: harmonic vibrator model. The numbers in brackets indicate the errors of varied parameters in the last digit.

Last column: E = exchange; MI = macroscopic imaginary potential; dC = deformed Coulomb potential.

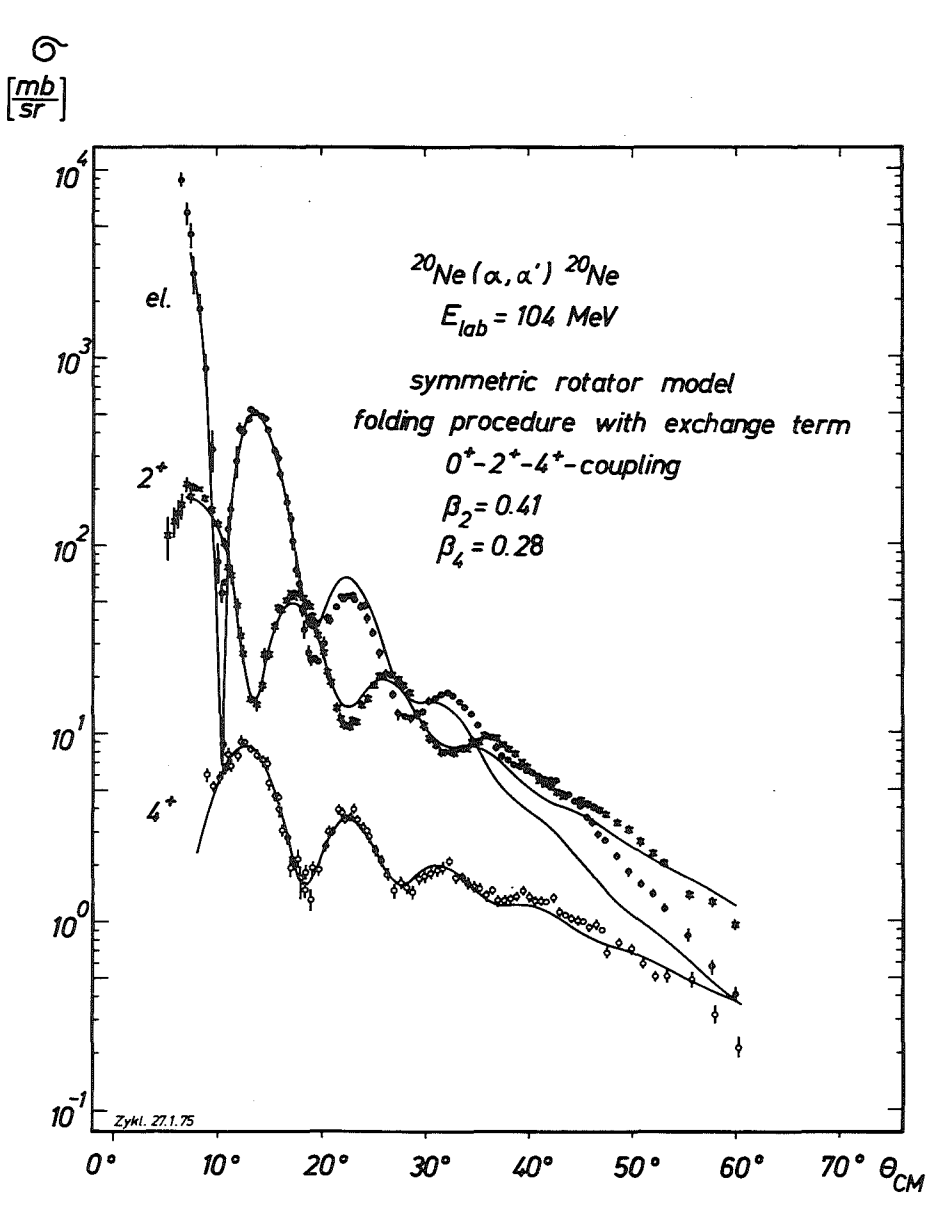

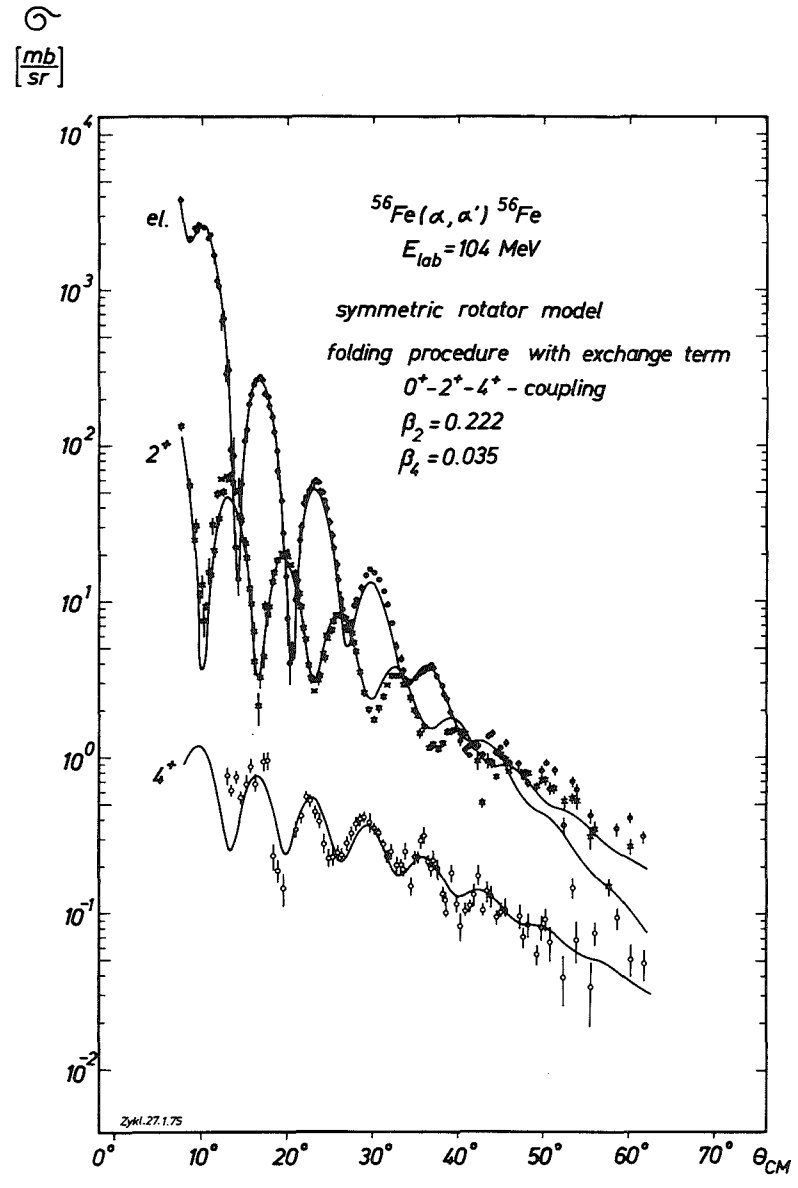

Fig. 5 Coupled channel analysis of inelastic scattering including the exchange term
a) ^{20}Ne, ^{56}Fe; symmetric rotator model.

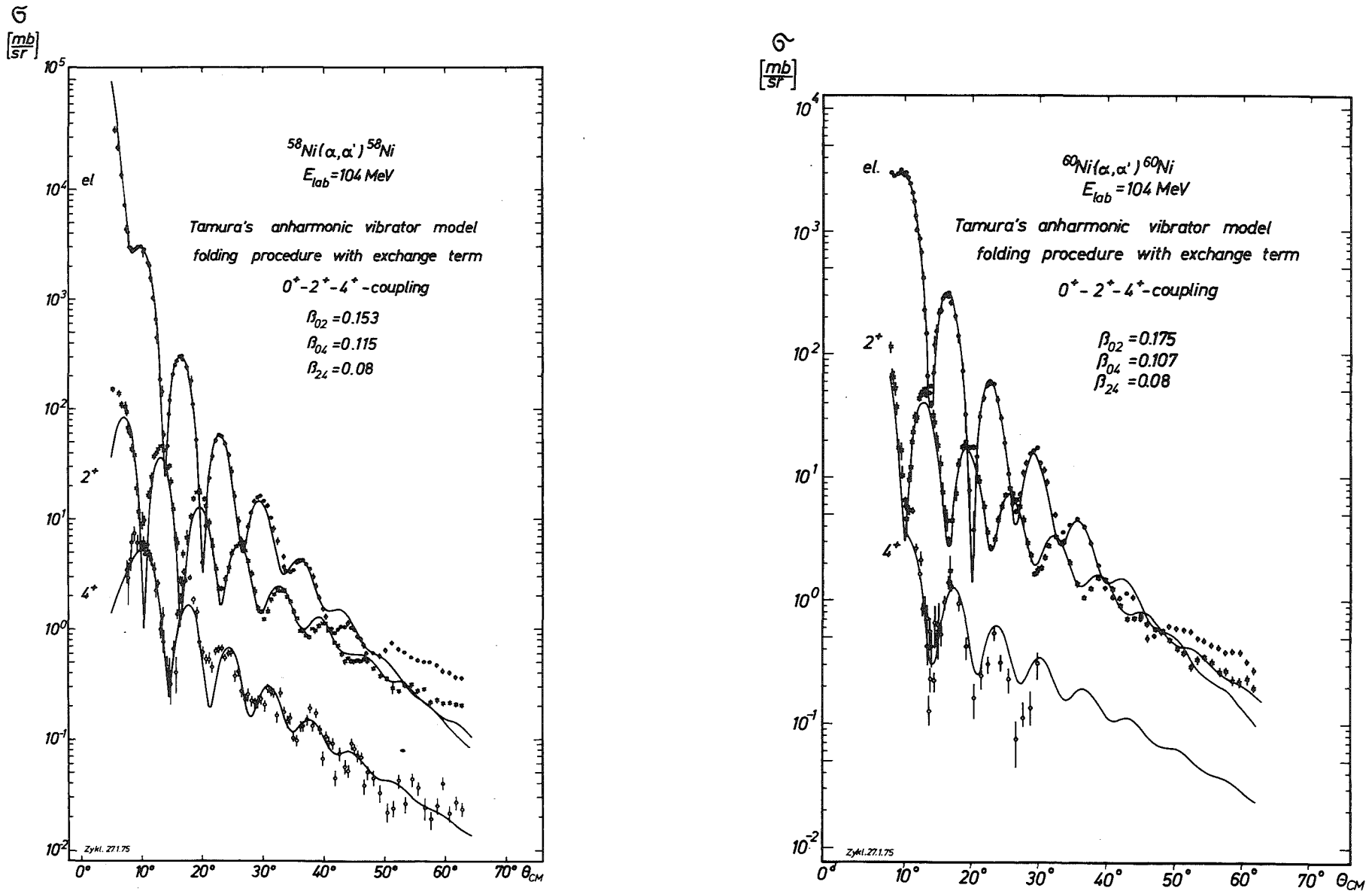

Fig. 5 b ^{58}Ni, ^{60}Ni anharmonic vibrator model |Ta 65, 66, Re Lö 72 a|

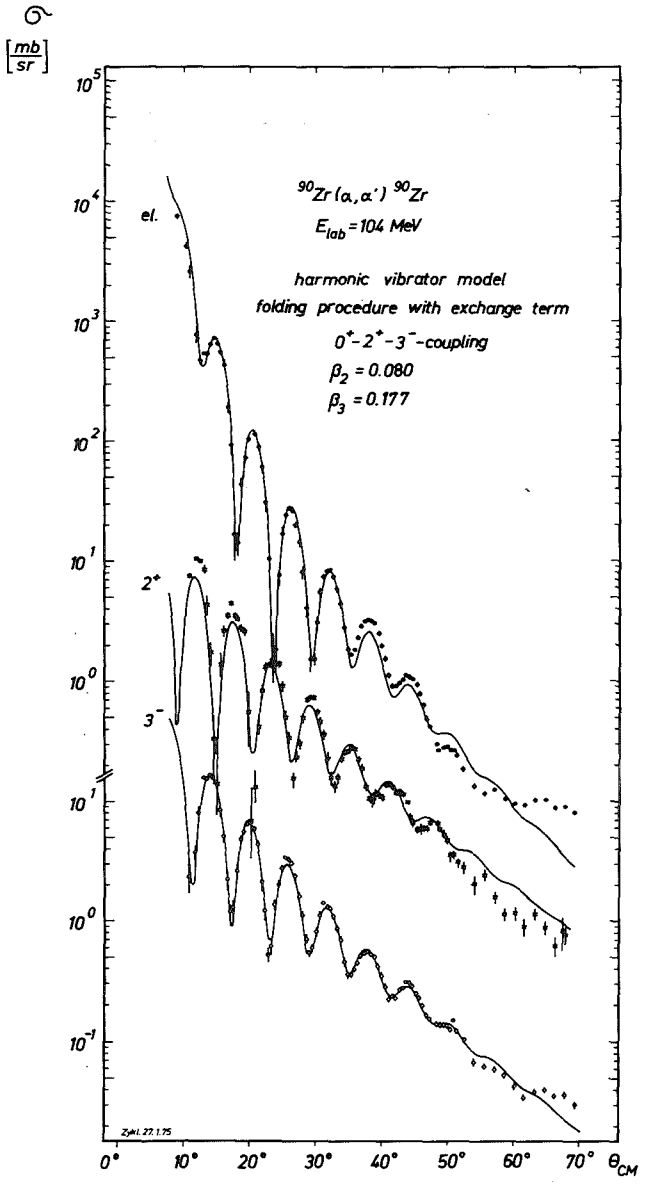

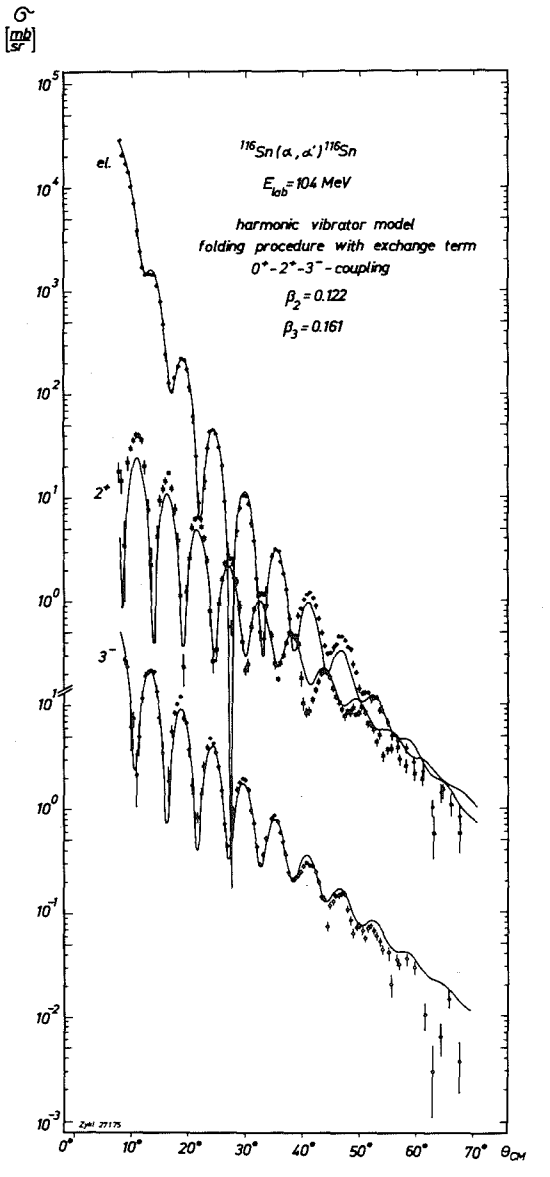

Fig. 5 c ^{90}Zr, ^{116}Sn harmonic quadrupole-octupole vibrator model

reproduce the radial behaviour of the potential in the surface region (4-7 fm) (see fig. 6).

In further calculations the effect of choosing the macroscopic Saxon-Woods representation of the (deformed) imaginary potential is studied. As demonstrated by two examples the best fit values of the parameters of the deformed Fermi distribution ρ_m are slightly different from those obtained by the different procedure, yet the values of the quadrupole moment and of the transition probability remain nearly unchanged (imaginary potential $U_I = \lambda_I/\lambda_R \cdot U_R$: $Q_{20} = 99.7 \pm 2.8$ e fm^2, U_I with independent geometry: $Q_{20} = 97.9 \pm 3.7$ e fm^2).

In fig. 7 the sensitivity of the measured cross sections to the size and shape parameters is illustrated for the case of the scattering from ^{56}Fe. By very extensive coupled channel calculations contour plots of the χ^2-values in the various parameter planes around the minimum value χ^2_{min} have been determined. As already found in elastic scattering |Gi Re 74 a| the cross sections are less sensitive to the particular choice of c_m and a_m provided that the combination reproduces the correct value of the rms-radius. Similar correlations are found between c_m, a_m and the deformation parameters. (The various curves in fig. 7 represent sections through the χ^2-minimum point enveloped by the hyper surface $\chi^2 = 2 \cdot \chi^2_{min}$ in the multi dimensional parameter space). While the deformation parameters less affect the rms-radius value they distinctly influence the Q_{20} value, which is rather well defined by the inelastic cross sections. The rms-radius and the intrinsic quadrupole moment seem to be the two independent quantities which determine the cross sections.

Finally we deduce isoscalar transition rates B(IS L; 0 → L) from the results of tab. 7 (without exchange term). On the basis of the rotational model these rates are given by

$$(4.1) \qquad B(IS\ L;\ 0 \rightarrow L) = \frac{2L+1}{16\pi}\ Q^2_{L0}$$

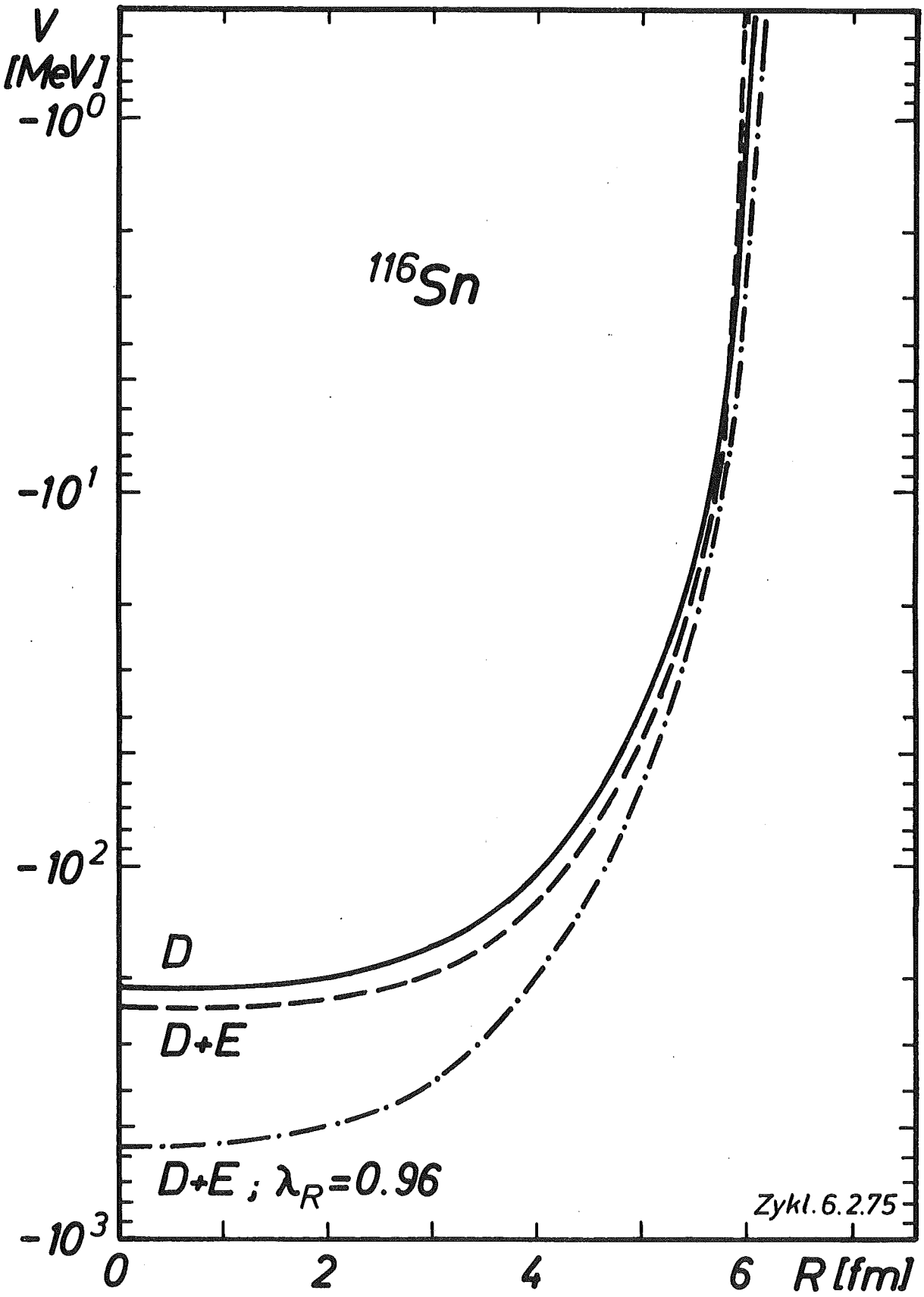

Fig. 6 Real central potential of ^{116}Sn inelastic scattering analyses (see tab. 6 line 16-18)
D = direct term only; D+E direct plus exchange term
D+E; λ_R = 0.96 direct plus exchange term, λ_R mismatch.

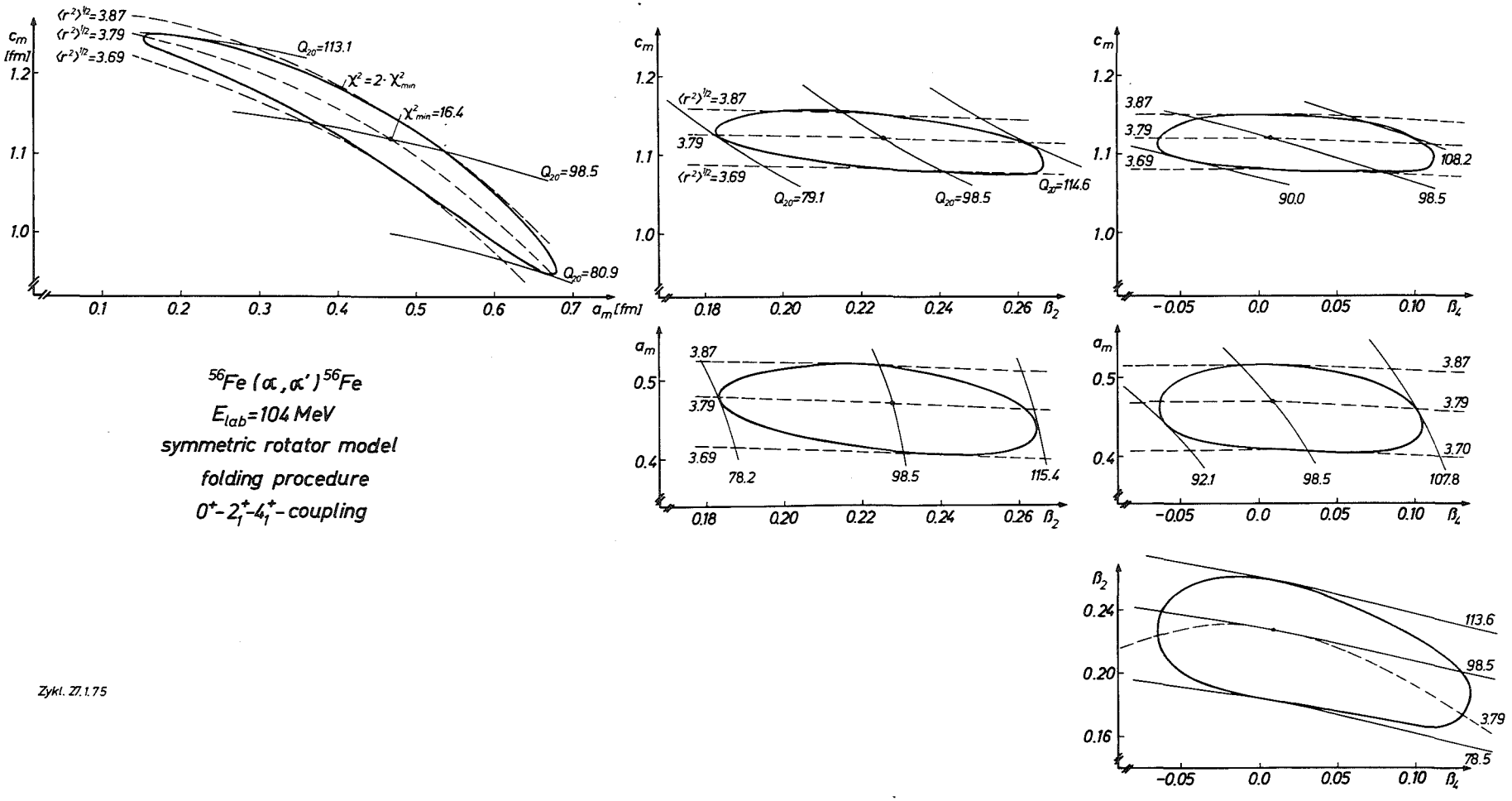

Fig. 7 ^{56}Fe: Contour plots of the χ^2-values in the various parameter planes around the minimum χ^2-value.

with

$$Q_{LO} = \frac{Z}{A}\sqrt{\frac{16\pi}{2L+1}} \int \rho_m(\vec{r}) \cdot Y_{LO}\, r^{L+2}\, dr\, d\Omega$$

In the vibrational case the reduced transition rates are calculated via the expression

$$(4.2) \quad B(IS\,L;\, 0 \to L) = \left(\frac{Z}{A} \cdot \left| f^{(1)} \langle 0||Q_L^{(1)}||I\rangle + f^{(2)}\langle 0||Q_L^{(2)}||I\rangle \right|\right)^2$$

with the radial form factors

$$f^{(1)} = c_{m_o} \int r^4 \frac{\delta\rho}{\delta c_{m_o}}\, dr \text{ and } f^{(2)} = c_{m_o}^2 \int r^4 \frac{\delta^2\rho}{\delta c_{m_o}^2}\, dr$$

The first order matrix elements $\langle 0||Q_L^{(1)}||I\rangle$ are identical with the β_L-values while the second order terms depend on details of the anharmonicities of the vibrational model. For the $0^+ \to 2_1^+$ transition the second order matrix element

$$\langle 0||Q_2^{(2)}||2_1\rangle = \frac{1}{\sqrt{4\pi}} \left(\sqrt{2}\, b_1\, \beta_2^2 \langle 2200|20\rangle + c_1\beta_2\beta_4\langle 2400|20\rangle\right)$$

depends on the two phonon admixture (b_1) and the one hexadecapole phonon admixture (c_1) to the first 2^+ state (see| Re Lö 72 a|). In the cases where we apply the vibrational model these amplitudes are expected to be very small so that for the $0 \to 2_1^+$ transition second order terms are neglected.+) In the same way the octupole transition rate is calculated only in first order. For a $0^+ \to 4_1^+$ transition however second order contributions are certainly of importance as in the matrix elements

$$\langle 0||Q_4^{(2)}||4_1\rangle = \frac{1}{\sqrt{4\pi}} \left(\sqrt{2}\, b_4\beta_2^2 \langle 2200|40\rangle + c_4\beta_2\beta_4\langle 2400|40\rangle\right)$$

the amplitude $b_4 (\approx \beta_{24}/\beta_{02})$ has the order of magnitude of 1. The amplitude c_4 is expected to be small and a corresponding contribution is omitted. For the calculation of the transition rates the c_m values quoted in tab. 7 have been converted into values c_{nm} of the nuclear mass distribution by the procedure

+) The amplitude b_1 is related to the static quadrupole moment by $Q_2 = \frac{12}{5}\frac{1}{\sqrt{7\pi}} b_1 \cdot Z \cdot c_{m_o}^2 \cdot \beta_2$, so that second order effects would certainly contribute in applying the expression 4.2 to deformed nuclei.

Nuclide	$B(IS\ 2;\ 0^+ \to 2_1^+)$ $[e^2 \cdot fm^4]$	$B(IS\ 2;\ 0^+ \to 2_1^+)$ s.p.u.	$B(E2;\ 0^+ \to 2_1^+)$ s.p.u.	Reference	Method
^{20}Ne	323. (20.)	20. (1.3)	20. (3.8)	[St Gr 65, Be 69]+	EM
			19.3 (3.0)	[Ko Fu 66, Be 69]+	IS
			14.7 (2.3)	[Sp Ha 65, Be 69]+	IS
^{56}Fe	1095. (75.)	17.2(1.2)	14.1 (1.6)	[St Gr 65, Be 69]+	EM
			15.2 (0.3)	[Le Cl 72]	EM reorientation
			12.4 (1.9)	[Be 69]	IS
^{58}Ni	484. (39.)	7.3(0.6)	9.9 (1.5)	[Du Bo 67, Be 69]+	EM Coulomb excit.
			10.3 (0.2)	[Le Cl 70]	EM reorientation
			15.8 (1.6)	[Ja Ha 67, Be 69]+	IS
^{60}Ni	696. (45.)	10.6(0.6)	14.0 (1.2)	[St Gr 65, Be 69]+	EM
			13.1 (0.3)	[Cl Ge 69]	EM reorientation
			20.0	[In 68, Be 69 +]	IS
^{90}Zr	446. (24.)	3.72(0.2)	3.5 (1.3)	[St Gr 65, Be 69]+	EM
			5.7 (1.7)	[Ma Be 68]	IS
^{116}Sn	2374. (68.)	14.1 (0.4)	14.0 (0.7)	[St 68, Be 69]+	EM
			17.0 (2.5)	[Bi Ha 68, Be 69]+	IS
	$B(IS\ 3;\ 0^+ \to 3_1^-)$ $[e^2 \cdot fm^6] \cdot 10^{-3}$	$B(IS\ 3;\ 0^+ \to 3_1^-)$ s.p.u.	$B(E3;\ 0^+ \to 3_1^-)$ s.p.u.		
^{56}Fe	19.8 (2.1)	15.2 (2.5)++	4.8	[Be 69]	IS
^{90}Zr	69.4 (3.8)	20.6 (2.2)	20.0 (1.6)	[Ma Be 68]	IS
^{116}Sn	157.6 (5.4)	28.2 (0.9)	15. (4.)	[Cu 68, Be 69]+	EM
			24.2 (3.6)	[Bi Ha 68, Be 69]+	IS
	$B(IS\ 4;\ 0^+ \to 4_1^+)$ $[e^2 \cdot fm^8] \cdot 10^{-4}$	$B(IS\ 4;\ 0^+ \to 4_1^+)$ s.p.u.	$B(E4;\ 0^+ \to 4_1^+)$ s.p.u.		
^{20}Ne	7.9 (1.2)	47.6 (7.2)			
^{56}Fe	7.6 (1.8)	2.9 (0.5)			
^{58}Ni	22.3 (2.6)	7.8 (1.)	4.5 (1.0)	[Ja Ha 67]	IS
^{60}Ni	19.3 (2.3)	6.9 (0.7)			

+ Quoted values were taken from [Be 69]

++ The analysis of our data basing on the harmonic vibrator model resulted in $\beta_3 = 0.228$

Tab. 8 Isoscalar transition rates B(IS L; 0 → L) calculated from the results quoted in tab. 7, by the method given in the text. Column 4-6 show comparable experimental results obtained by various methods. Numbers in bracket indicate the errors in the last digits.

used in sect. 2.1. In Tab. 8 the results are compiled and compared to findings obtained by different methods.

5. CONCLUDING REMARKS

The presented empirical studies of the effective interaction in the folding model approach of 104 MeV α-particle scattering results in the following statements:

(i) Elastic scattering differential cross sections in particular in the diffraction region can well be described by a Gaussian effective interaction the strength of which phenomenogolically was adjusted to 0.96 · 43. MeV for 104 MeV α-particles. The resulting rms-radii of nuclear matter are in agreement with comparable values of the charge distribution, except for very light nuclei, for which the adopted form of the density distribution may not be reasonable.

(ii) The effective interaction obtained from elastic scattering can be applied to coupled channel calculations of the inelastic scattering without further modification. RMS-radii and multipole moments of the nucleon density distribution are unambigously defined by the measured cross sections though some parameter correlations exist.

(iii) Exchange effects frequently discussed [Bi Ta 73, Schae 70] need not to be explicitely considered because their influence is sufficiently absorbed by the phenomenologically adjusted strength of the effective interaction.

Furthermore a method for deducing isoscalar transition rates from (α,α') reactions is proposed in this paper. It is directly based on the nucleon density distribution the parameter values of which were obtained from a folding model fit to the measured data. This procedure is more closely related to the induced transitions which are considered to be due to rotations or vibrations of the nuclear matter distribution. Therefore this method seems to be

more reasonable than those approaches |Be 69| which are primarily based on parameters of a deformed optical potential extracted from ordinary DWBA analyses.

ACKNOWLEDGEMENT

The authors are indebted to Dr. G.W. Schweimer for many clarifying discussions in particular concerning the computer code ECIS Karlsruhe. We thank Dr. G. Schatz for his encouraging interest in our studies.

REFERENCES

Ba Fr 71 — C.J. Batty, E. Friedmann and D.F. Jackson; Nucl. Phys. A 175 (1971) 1

Be 69 — A.M. Bernstein; Advances in Nuclear Physics, Vol. 3 ed. M. Baranger and E. Vogt, (Plenum Press, New York, London, 1969) p. 325

Be Se 71 — A.M. Bernstein and W.A. Seidler; Phys. Lett. 34 B (1971) 569

Be Se 72 — A.M. Bernstein and W.A. Seidler, Phys. Lett. 39 B (1972) 583

Bi Ha 68 — C.R. Bingham and M.L. Halbert, O.R.N.L. 4217(1968)

Bi Ta 73 — L. Bimbot, B. Tatischeff, I. Brissaud, Y. Le Bornec, N. Frascaria and A. Willis; Nucl. Phys. A 210 (1973)397

Br Bo 72 — I. Brissaud, Y. Le Bornec, B. Tatischeff, L. Bimbot, M.K. Brussel et G. Duhamel; Nucl. Phys. A 191 (1972)145

Bu Du 70 — A. Budzanowski, A. Dudek, K. Grotowski, A. Strzalkowski; Phys. Lett. 32 B (1970) 431

Cl Ge 69 — D. Cline, H.S. Gertzman, H.E. Gove, P.M.S. Lesser and J.J. Schwartz; Nucl. Phys. A 133 (1969)445

Cu 68 — T.H. Curtis; Ph. D. Thesis, Yale University (1968)

Du Bo 67 — M.A. Duguay, C.K. Bockelman, T.H. Curtis; and R.A. Eisenstein; Phys. Rev. 163 (1967) 1259

El 61 — L.R.B. Elton; "Nuclear Sizes", Oxford University Press, London (1961)

Fr Ho 68 — R.F. Frosch, R. Hofstadter, J.S. McCarthy, G.K. Nöldeke, K.J. van Oostrum, M.R. Yearian, B.C. Clark, R. Herman and D.G. Ravenhall; Phys. Rev. 174 (1968) 1380

Gi Re 74 a — H.J. Gils, H. Rebel, G. Nowicki, D. Hartmann, A. Ciocănel, H. Klewe-Nebenius, K. Wisshak; Report KFK 2087, Kernforschungszentrum Karlsruhe (1974)

Gi Re 74 b — H.J. Gils, H. Rebel and A. Ciocănel, Rev. Roum. de Phys. 19 (1974) 761

Gl Ve 66 — N.K.Glendenning and M. Veneroni, Phys. Rev. 144 (1966)839

Ha Ha 70 — D. Habs, G. Hauser, Gudrun Hoffmann, H. Klewe-Nebenius, R. Löhken, Uta Martens, H. Rebel, G. Schatz, G.W. Schweimer, J. Specht; External report 18/70-2, Kernforschungszentrum Karlsruhe (1970) unpublished

Ha Lö 69 — G. Hauser, R. Löhken, H. Rebel, G. Schatz, G.W. Schweimer and J. Specht; Nucl. Phys. A 128 (1969) 81

Ho Co 67 — R. Hofstadter and H.R. Collard; Landolt-Börnstein, Neue Serie, Group I. Vol. 2, Springer-Verlag, Berlin, Heidelberg, New York (1967)

In 68 — M. Inone; Nucl. Phys. A 119 (1968) 449

Ja 70 — D.F. Jackson; Phys. Lett. 32 B (1970) 233

Ja Ha 67 — O.N. Jarvis, B.G. Harvey, D.L. Hendrie and J. Mahoney; Nucl. Phys. A 102 (1967) 625

Ja Ke 69 — D.F. Jackson and V.K. Kembhavi; Phys. Rev. 178 (1969) 1626

Ko Fu 66 — J. Kokame, F. Fukunaga, and H. Nakamura; Proceedings of the International Conference on Nuclear Physics, Gatlinburg, Tennessee (1966).

Le Cl 72 — P.M.S. Lesser, D. Cline, Philip Goode and R.N. Horoshko; Nucl. Phys. A 190 (1972) 597

Le Hi 72 — G.M. Lerner, J.C. Hiebert, L.L. Rutledge and A.M. Bernstein; Phys. Rev. C6 (1972) 1254

Ma Be 68 — E.J. Martens and A.M. Bernstein; Nucl. Phys. A 117 (1968) 241, Phys. Lett. 24 B (1967)669

Ma Li 73 — P. Mailandt, J.S. Lilley and G.W. Greenless; Phys. Rev. C8 (1973) 2189

Mo Ja 69 — C.G. Morgan and D.F. Jackson; Phys. Rev. 188 (1969)1785

Re 74 — H. Rebel; Report KFK 2065 (1974) Kernforschungszentrum Karlsruhe

Re Ha 74 — H. Rebel, G. Hauser, G.W. Schweimer, G. Nowicki, W. Wiesner and D. Hartmann; Nucl. Phys. A 218 (1974)13

Re Lö 72 a — H. Rebel, R. Löhken, G.W. Schweimer, G. Schatz and G. Hauser; Z. Phys. 256 (1972) 258.

Re Sc 72 b — H. Rebel, G.W. Schweimer, G. Schatz, J. Specht, R. Löhken, G. Hauser, D. Habs and H. Klewe-Nebenius; Nucl. Phys. A 182 (1972) 145

Re Ta 70	I. Reichstein and Y.C. Tang; Nucl. Phys. A 158 (1970) 529
Sa 71	G.R. Satchler; Nuclei and Particles 2 (1971) 265
Scha 70	R. Schaeffer; Nucl. Phys. A 158 (1970) 321
Sc Ra 73	G.W. Schweimer and J. Raynal; preprint (1973) and private communications
Sp Ha 65	A. Springer and B.G. Harvey; Phys. Lett. 14 (1965) 116, 316
St Gr 65	P.H. Stelson and L. Grodzins; Nuclear Data 1 (1965) 21
St 68	P.H. Stelson, F.K. McGowan, R.L. Robinson, W.T. Milner and. R.O. Sayer; Phys. Rev. 170 (1968) 1172
Ta 65	T. Tamura; Rev. Mod. Phys. 37 (1965) 679
Ta 66	T. Tamura; Progr. Theor. Phys. Suppl. 37, 38 (1966) 198
Ta 72	T. Tamura; Z. Phys. 256 (1972) 1258
Tas 73	L.J. Tassie, Austral. J. Phys. 26 (1973) 433

Appendix

Experimental cross sections of ^{90}Zr and ^{116}Sn: The quoted errors of the experimental cross sections include the error arising from the finite angular acceptance which is converted into a cross section error.

SCATTERING OF 104 MEV ALPHAPARTICLES ON 90 ZR

Q = 0.0 MEV I = 0+

ECM = 99.573 MEV K = 4.2724/FERMI ETA = 2.47120

LABORATORY DATA			RUTHERFORD	CM DATA		
THETA DEGREE	SIGMA MB/SR	DSIGMA %	SIGMA/SR	THETA DEGREE	SIGMA MB/SR	DSIGMA MB/SR
8.55	8.262E+03	3.1	3.335E-01	8.94	7.564E+03	2.318E+02
9.95	4.720E+03	6.6	3.490E-01	10.40	4.323E+03	2.645E+02
10.45	2.879E+03	9.9	2.588E-01	10.92	2.637E+03	2.618E+02
11.45	8.431E+02	16.0	1.091E-01	11.97	7.725E+02	1.238E+02
11.95	5.105E+02	5.3	7.835E-02	12.49	4.678E+02	2.471E+01
12.55	5.867E+02	1.1	1.095E-01	13.12	5.377E+02	6.036E+00
12.95	5.843E+02	2.0	1.235E-01	13.54	5.356E+02	1.061E+01
13.45	7.017E+02	2.9	1.725E-01	14.06	6.433E+02	1.856E+01
13.95	7.857E+02	0.3	2.234E-01	14.58	7.205E+02	2.389E+00
14.45	7.161E+02	2.5	2.342E-01	15.10	6.568E+02	1.620E+01
14.95	6.103E+02	5.7	2.285E-01	15.62	5.599E+02	3.190E+01
15.45	3.690E+02	10.8	1.575E-01	16.15	3.386E+02	3.640E+01
15.95	2.139E+02	12.5	1.036E-01	16.67	1.963E+02	2.460E+01
16.45	1.014E+02	19.3	5.552E-02	17.19	9.308E+01	1.798E+01
16.95	1.817E+01	47.3	1.121E-02	17.71	1.668E+01	7.897E+00
17.45	1.541E+01	18.6	1.067E-02	18.23	1.415E+01	2.631E+00
17.95	4.666E+01	13.9	3.613E-02	18.76	4.286E+01	5.944E+00
18.45	7.991E+01	8.4	6.859E-02	19.28	7.342E+01	6.182E+00
18.95	1.139E+02	4.1	1.093E-01	19.80	1.047E+02	4.311E+00
19.45	1.266E+02	1.0	1.347E-01	20.32	1.164E+02	1.110E+00
19.95	1.251E+02	2.3	1.472E-01	20.84	1.150E+02	2.624E+00
20.45	9.853E+01	6.1	1.279E-01	21.36	9.062E+01	5.492E+00
20.95	6.555E+01	9.9	9.362E-02	21.89	6.031E+01	5.944E+00
21.45	3.397E+01	16.0	5.326E-02	22.41	3.126E+01	4.987E+00
21.95	1.142E+01	26.2	1.961E-02	22.93	1.051E+01	2.966E+00
22.45	1.791E+00	52.7	3.362E-03	23.45	1.649E+00	8.688E-01
22.95	1.995E+00	33.2	4.085E-03	23.97	1.838E+00	6.104E-01
23.45	8.401E+00	19.5	1.873E-02	24.49	7.741E+00	1.510E+00
23.95	1.837E+01	9.7	4.450E-02	25.01	1.693E+01	1.649E+00
24.45	2.623E+01	4.3	6.894E-02	25.53	2.418E+01	1.050E+00
24.95	2.963E+01	0.9	8.434E-02	26.05	2.733E+01	2.511E-01
25.45	2.831E+01	2.8	8.712E-02	26.57	2.612E+01	7.315E-01
25.95	2.189E+01	5.9	7.272E-02	27.09	2.020E+01	1.185E+00
26.45	1.556E+01	8.5	5.572E-02	27.61	1.437E+01	1.222E+00
26.95	8.712E+00	12.9	3.358E-02	28.14	8.046E+00	1.036E+00
27.45	4.367E+00	16.2	1.809E-02	28.66	4.035E+00	6.547E-01
27.95	1.657E+00	16.5	7.368E-03	29.18	1.531E+00	2.534E-01
28.45	1.656E+00	10.4	7.893E-03	29.70	1.531E+00	1.593E-01
28.95	3.336E+00	12.9	1.702E-02	30.22	3.085E+00	3.991E-01
29.45	5.929E+00	8.0	3.235E-02	30.74	5.486E+00	4.407E-01
29.95	8.033E+00	3.8	4.682E-02	31.26	7.435E+00	2.813E-01
30.45	8.848E+00	1.6	5.501E-02	31.78	8.193E+00	1.297E-01
30.95	9.087E+00	1.5	6.021E-02	32.29	8.418E+00	1.261E-01
31.45	7.862E+00	3.7	5.545E-02	32.81	7.286E+00	2.730E-01
31.95	6.254E+00	5.1	4.691E-02	33.33	5.798E+00	2.970E-01
32.45	4.712E+00	6.9	3.754E-02	33.85	4.370E+00	3.034E-01
32.95	3.023E+00	9.2	2.556E-02	34.37	2.805E+00	2.572E-01
33.45	1.960E+00	6.5	1.757E-02	34.89	1.819E+00	1.191E-01
33.95	1.786E+00	2.0	1.696E-02	35.41	1.659E+00	3.325E-02
34.45	1.970E+00	4.0	1.980E-02	35.93	1.830E+00	7.273E-02
34.95	2.518E+00	4.7	2.677E-02	36.45	2.340E+00	1.093E-01
35.45	3.102E+00	3.3	3.484E-02	36.97	2.885E+00	9.560E-02
35.95	3.416E+00	1.4	4.050E-02	37.49	3.178E+00	4.554E-02
36.45	3.447E+00	1.0	4.311E-02	38.00	3.208E+00	3.252E-02
36.95	3.377E+00	1.6	4.452E-02	38.52	3.145E+00	5.029E-02
37.45	3.211E+00	2.4	4.458E-02	39.04	2.992E+00	7.231E-02
37.95	2.663E+00	4.4	3.891E-02	39.56	2.482E+00	1.091E-01
38.45	2.086E+00	5.1	3.206E-02	40.08	1.945E+00	9.857E-02
38.95	1.644E+00	5.6	2.655E-02	40.59	1.534E+00	8.596E-02
39.45	1.191E+00	5.9	2.020E-02	41.11	1.112E+00	6.562E-02
39.95	9.718E-01	3.0	1.730E-02	41.63	9.076E-01	2.756E-02
40.45	9.630E-01	1.8	1.798E-02	42.15	8.998E-01	1.638E-02
40.95	1.035E+00	2.1	2.026E-02	42.66	9.676E-01	1.996E-02
41.45	1.115E+00	2.0	2.286E-02	43.18	1.043E+00	2.066E-02
41.95	1.192E+00	1.2	2.559E-02	43.70	1.116E+00	1.284E-02
42.45	1.159E+00	1.6	2.603E-02	44.21	1.085E+00	1.729E-02
42.95	1.103E+00	2.0	2.590E-02	44.73	1.033E+00	2.114E-02
43.45	9.981E-01	3.0	2.449E-02	45.25	9.356E-01	2.765E-02
43.95	8.349E-01	4.6	2.140E-02	45.76	7.830E-01	3.605E-02
44.45	6.673E-01	5.1	1.786E-02	46.28	6.262E-01	3.184E-02
44.95	5.172E-01	4.5	1.444E-02	46.80	4.856E-01	2.180E-02
45.45	4.513E-01	3.4	1.314E-02	47.31	4.240E-01	1.459E-02
46.45	3.169E-01	3.8	1.002E-02	48.35	2.980E-01	1.120E-02
46.95	2.861E-01	2.4	9.418E-03	48.86	2.692E-01	6.396E-03
47.45	2.994E-01	2.3	1.026E-02	49.38	2.819E-01	6.517E-03
47.95	3.082E-01	2.3	1.058E-02	49.89	2.904E-01	6.654E-03
48.45	2.826E-01	2.4	1.047E-02	50.41	2.664E-01	6.400E-03
48.95	2.848E-01	2.4	1.057E-02	50.92	2.686E-01	6.571E-03
49.45	2.592E-01	3.1	1.037E-02	51.44	2.446E-01	7.705E-03
50.45	1.999E-01	4.1	8.621E-03	52.47	1.889E-01	7.653E-03
51.95	1.397E-01	5.7	6.721E-03	54.01	1.322E-01	7.567E-03
53.45	1.240E-01	3.5	6.631E-03	55.55	1.176E-01	4.127E-03
54.95	1.330E-01	3.2	7.879E-03	57.09	1.264E-01	4.090E-03
56.45	1.104E-01	3.3	7.221E-03	58.63	1.051E-01	3.511E-03
57.95	1.000E-01	3.4	7.200E-03	60.17	9.540E-02	3.288E-03
59.45	9.698E-02	3.8	7.665E-03	61.70	9.271E-02	3.551E-03
60.95	1.062E-01	3.2	9.187E-03	63.24	1.017E-01	3.275E-03
62.45	1.068E-01	3.3	1.009E-02	64.77	1.025E-01	3.392E-03
63.95	9.129E-02	3.5	9.387E-03	66.30	8.781E-02	3.033E-03
65.45	9.130E-02	3.5	1.020E-02	67.83	8.801E-02	3.065E-03
66.95	8.475E-02	3.8	1.026E-02	69.36	8.188E-02	3.121E-03
68.45	7.047E-02	3.9	9.222E-03	70.88	6.823E-02	2.670E-03
69.95	6.785E-02	4.8	9.580E-03	72.41	6.584E-02	3.191E-03
71.45	5.843E-02	5.6	8.882E-03	73.93	5.682E-02	3.182E-03
72.95	5.029E-02	5.6	8.214E-03	75.45	4.902E-02	2.724E-03

SCATTERING OF 104 MEV ALPHAPARTICLES ON 90 ZR

Q = -2.186 MEV I = 2+

ECM = 97.387 MEV K = 4.2252/FERMI ETA = 2.43878

LABORATORY DATA			CM DATA		
THETA DEGREE	SIGMA MB/SR	DSIGMA %	THETA DEGREE	SIGMA MB/SR	DSIGMA MB/SR
10.45	8.136E+00	5.8	10.93	7.445E+00	4.281E-01
11.45	1.167E+01	2.9	11.97	1.068E+01	3.115E-01
11.95	1.098E+01	3.3	12.50	1.005E+01	3.350E-01
12.45	9.402E+00	8.8	13.02	8.605E+00	7.549E-01
12.95	4.726E+00	18.9	13.54	4.328E+00	8.162E-01
13.45	1.928E+00	24.3	14.06	1.766E+00	4.292E-01
13.95	3.610E-01	59.4	14.59	3.307E-01	1.965E-01
14.45	1.522E-01	104.8	15.11	1.395E-01	1.462E-01
14.95	1.502E+00	21.1	15.63	1.377E+00	2.902E-01
15.45	2.843E+00	9.7	16.15	2.606E+00	2.540E-01
15.95	3.823E+00	6.9	16.68	3.505E+00	2.420E-01
16.45	4.834E+00	4.1	17.20	4.433E+00	1.826E-01
16.95	3.859E+00	5.4	17.72	3.540E+00	1.910E-01
17.45	3.660E+00	5.2	18.24	3.358E+00	1.746E-01
17.95	3.038E+00	6.2	18.76	2.788E+00	1.716E-01
18.45	2.828E+00	9.2	19.29	2.596E+00	2.377E-01
18.95	6.036E-01	47.2	19.81	5.542E-01	2.618E-01
19.45	7.416E-02	95.2	20.33	6.811E-02	6.481E-02
19.95	1.432E-01	40.5	20.85	1.316E-01	5.334E-02
20.45	4.666E-01	18.6	21.37	4.288E-01	7.969E-02
20.95	9.053E-01	11.9	21.90	8.322E-01	9.906E-02
21.45	1.453E+00	5.7	22.42	1.336E+00	7.607E-02
21.95	1.480E+00	4.3	22.94	1.361E+00	5.808E-02
22.45	1.622E+00	4.0	23.46	1.492E+00	6.034E-02
22.95	1.842E+00	2.6	23.98	1.695E+00	4.466E-02
23.45	1.486E+00	6.4	24.50	1.368E+00	8.775E-02
23.95	9.971E-01	10.3	25.02	9.182E-01	9.435E-02
24.45	5.429E-01	12.9	25.54	5.001E-01	6.447E-02
24.95	3.709E-01	12.4	26.06	3.418E-01	4.253E-02
25.45	1.667E-01	15.3	26.59	1.537E-01	2.352E-02
25.95	2.580E-01	10.4	27.11	2.379E-01	2.470E-02
26.45	3.283E-01	11.1	27.63	3.028E-01	3.347E-02
26.95	5.409E-01	9.5	28.15	4.991E-01	4.720E-02
27.45	7.682E-01	5.0	28.67	7.091E-01	3.574E-02
27.95	7.805E-01	4.0	29.19	7.207E-01	2.847E-02
28.45	7.849E-01	4.3	29.71	7.251E-01	3.111E-02
28.95	5.999E-01	6.7	30.23	5.544E-01	3.741E-02
29.45	4.985E-01	6.8	30.75	4.609E-01	3.121E-02
29.95	3.901E-01	8.7	31.27	3.608E-01	3.132E-02
30.45	2.464E-01	12.2	31.79	2.280E-01	2.788E-02
30.95	1.680E-01	12.3	32.31	1.555E-01	1.908E-02
31.45	1.455E-01	10.5	32.83	1.347E-01	1.412E-02
31.95	1.714E-01	9.6	33.35	1.588E-01	1.517E-02
32.45	2.459E-01	6.9	33.87	2.279E-01	1.579E-02
32.95	2.762E-01	4.4	34.39	2.561E-01	1.116E-02
33.45	2.817E-01	4.3	34.91	2.613E-01	1.135E-02
33.95	3.104E-01	5.5	35.43	2.880E-01	1.570E-02
34.45	2.937E-01	4.7	35.95	2.727E-01	1.282E-02
34.95	2.390E-01	5.9	36.46	2.220E-01	1.312E-02
35.45	2.035E-01	8.6	36.98	1.891E-01	1.624E-02
35.95	1.424E-01	9.0	37.50	1.324E-01	1.188E-02
36.45	1.130E-01	7.9	38.02	1.051E-01	8.295E-03
36.95	1.067E-01	10.0	38.54	9.928E-02	9.964E-03
37.45	1.239E-01	10.9	39.06	1.153E-01	1.253E-02
37.95	1.208E-01	6.7	39.58	1.125E-01	7.516E-03
38.45	1.180E-01	7.3	40.09	1.100E-01	8.009E-03
38.95	1.489E-01	5.6	40.61	1.388E-01	7.757E-03
39.45	1.520E-01	5.7	41.13	1.418E-01	8.044E-03
39.95	1.424E-01	6.1	41.65	1.329E-01	8.062E-03
40.45	1.280E-01	5.7	42.16	1.195E-01	6.829E-03
40.95	1.317E-01	5.0	42.68	1.230E-01	6.181E-03
41.45	1.234E-01	5.6	43.20	1.153E-01	6.429E-03
41.95	1.053E-01	6.7	43.72	9.849E-02	6.556E-03
42.45	7.955E-02	7.7	44.23	7.444E-02	5.711E-03
42.95	7.146E-02	7.1	44.75	6.690E-02	4.742E-03
43.45	6.201E-02	6.3	45.27	5.809E-02	3.669E-03
43.95	6.370E-02	10.3	45.78	5.970E-02	6.154E-03
44.45	6.387E-02	7.2	46.30	5.989E-02	4.335E-03
44.95	6.414E-02	6.0	46.82	6.018E-02	3.628E-03
45.45	7.153E-02	5.5	47.33	6.715E-02	3.693E-03
46.45	7.074E-02	5.4	48.37	6.649E-02	3.593E-03
46.95	6.259E-02	6.0	48.88	5.886E-02	3.544E-03
47.45	5.687E-02	6.8	49.40	5.351E-02	3.663E-03
47.95	5.088E-02	7.6	49.91	4.790E-02	3.632E-03
48.45	3.700E-02	9.1	50.43	3.486E-02	3.178E-03
48.95	3.783E-02	7.6	50.94	3.566E-02	2.705E-03
49.45	3.314E-02	8.2	51.46	3.126E-02	2.561E-03
50.45	2.936E-02	10.5	52.49	2.773E-02	2.919E-03
51.95	2.139E-02	17.7	54.03	2.024E-02	3.589E-03
53.45	2.569E-02	9.3	55.57	2.435E-02	2.274E-03
54.95	1.680E-02	11.6	57.11	1.596E-02	1.857E-03
56.45	1.176E-02	13.5	58.65	1.119E-02	1.510E-03
57.95	1.220E-02	12.5	60.19	1.163E-02	1.459E-03
59.45	9.476E-03	17.2	61.73	9.054E-03	1.561E-03
60.95	1.173E-02	13.2	63.26	1.123E-02	1.486E-03
62.45	9.057E-03	15.7	64.79	8.690E-03	1.368E-03
63.95	6.369E-03	19.3	66.32	6.124E-03	1.179E-03
65.45	7.882E-03	16.9	67.85	7.595E-03	1.280E-03
66.95	6.700E-03	20.2	69.38	6.470E-03	1.306E-03
68.45	7.516E-03	16.6	70.91	7.275E-03	1.207E-03
69.95	6.798E-03	21.2	72.43	6.594E-03	1.399E-03
71.45	5.643E-03	25.4	73.95	5.486E-03	1.392E-03
72.95	2.927E-03	43.0	75.48	2.852E-03	1.225E-03

SCATTERING OF 104 MEV ALPHAPARTICLES ON 90 ZR

Q = -2.748 MEV I = 3-

ECM = 96.825 MEV K = 4.2130/FERMI ETA = 2.50662

LABORATORY DATA THETA DEGREE	SIGMA MB/SR	DSIGMA %	CM DATA THETA DEGREE	SIGMA MB/SR	DSIGMA MB/SR
8.55	3.016E+01	5.7	8.94	2.758E+01	1.562E+00
10.45	2.551E+00	27.5	10.93	2.334E+00	6.429E-01
11.45	4.130E+00	14.2	11.98	3.780E+00	5.379E-01
11.95	8.801E+00	13.8	12.50	8.056E+00	1.112E+00
12.45	1.742E+01	4.7	13.02	1.595E+01	7.429E-01
12.95	1.671E+01	2.1	13.54	1.530E+01	3.142E-01
13.45	1.829E+01	2.0	14.07	1.675E+01	3.283E-01
13.95	1.761E+01	2.7	14.59	1.613E+01	4.401E-01
14.45	1.499E+01	6.0	15.11	1.373E+01	8.263E-01
14.95	9.181E+00	10.7	15.63	8.413E+00	9.028E-01
15.45	5.585E+00	12.6	16.16	5.119E+00	6.450E-01
15.95	2.447E+00	18.3	16.68	2.243E+00	4.106E-01
16.45	1.326E+00	11.5	17.20	1.216E+00	1.396E-01
16.95	1.415E+00	13.7	17.72	1.298E+00	1.773E-01
17.45	2.875E+00	14.3	18.24	2.637E+00	3.773E-01
17.95	5.275E+00	7.1	18.77	4.840E+00	3.440E-01
18.45	6.093E+00	3.7	19.29	5.592E+00	2.081E-01
18.95	7.198E+00	2.2	19.81	6.608E+00	1.459E-01
19.45	7.055E+00	1.9	20.33	6.478E+00	1.220E-01
19.95	6.449E+00	3.9	20.85	5.923E+00	2.337E-01
20.45	4.818E+00	7.7	21.38	4.427E+00	3.409E-01
20.95	2.889E+00	12.3	21.90	2.655E+00	3.262E-01
21.45	1.343E+00	17.8	22.42	1.235E+00	2.203E-01
21.95	5.811E-01	14.2	22.94	5.343E-01	7.568E-02
22.45	6.788E-01	14.6	23.46	6.244E-01	9.095E-02
22.95	1.498E+00	10.6	23.98	1.378E+00	1.462E-01
23.45	2.212E+00	7.3	24.50	2.036E+00	1.485E-01
23.95	3.029E+00	5.3	25.03	2.789E+00	1.484E-01
24.45	3.717E+00	2.3	25.55	3.423E+00	7.710E-02
24.95	3.571E+00	2.1	26.07	3.290E+00	6.884E-02
25.45	3.307E+00	3.5	26.59	3.048E+00	1.065E-01
25.95	2.584E+00	6.3	27.11	2.382E+00	1.497E-01
26.45	1.767E+00	8.1	27.63	1.630E+00	1.322E-01
26.95	1.217E+00	8.6	28.15	1.123E+00	9.670E-02
27.45	7.834E-01	9.0	28.67	7.230E-01	6.481E-02
27.95	5.813E-01	5.0	29.19	5.367E-01	2.671E-02
28.45	6.596E-01	6.0	29.71	6.092E-01	3.670E-02
28.95	8.855E-01	7.4	30.23	8.181E-01	6.018E-02
29.45	1.229E+00	6.0	30.75	1.136E+00	6.863E-02
29.95	1.529E+00	2.7	31.27	1.414E+00	3.885E-02
30.45	1.424E+00	2.9	31.79	1.317E+00	3.774E-02
30.95	1.386E+00	3.2	32.31	1.283E+00	4.122E-02
31.45	1.189E+00	4.6	32.83	1.101E+00	5.066E-02
31.95	9.473E-01	5.2	33.35	8.774E-01	4.538E-02
32.45	7.609E-01	6.4	33.87	7.050E-01	4.546E-02
32.95	5.050E-01	8.0	34.39	4.681E-01	3.724E-02
33.45	3.864E-01	5.0	34.91	3.583E-01	1.781E-02
33.95	3.930E-01	4.6	35.43	3.646E-01	1.690E-02
34.45	4.302E-01	3.8	35.95	3.993E-01	1.500E-02
34.95	4.854E-01	4.4	36.47	4.507E-01	1.970E-02
35.45	5.553E-01	4.2	36.99	5.159E-01	2.187E-02
35.95	5.848E-01	2.7	37.51	5.435E-01	1.457E-02
36.45	6.048E-01	2.5	38.02	5.624E-01	1.405E-02
36.95	5.650E-01	3.7	38.54	5.256E-01	1.967E-02
37.45	5.459E-01	3.1	39.06	5.081E-01	1.586E-02
37.95	4.578E-01	4.6	39.58	4.263E-01	1.971E-02
38.45	3.829E-01	5.1	40.10	3.567E-01	1.812E-02
38.95	3.072E-01	5.5	40.62	2.864E-01	1.587E-02
39.45	2.442E-01	4.5	41.13	2.277E-01	1.025E-02
39.95	2.581E-01	4.0	41.65	2.408E-01	9.542E-03
40.45	2.502E-01	3.7	42.17	2.336E-01	8.741E-03
40.95	2.920E-01	3.3	42.69	2.727E-01	8.922E-03
41.45	2.997E-01	3.3	43.20	2.801E-01	9.136E-03
41.95	3.420E-01	2.3	43.72	3.198E-01	7.496E-03
42.45	3.348E-01	2.7	44.24	3.132E-01	8.587E-03
42.95	3.144E-01	3.4	44.76	2.943E-01	1.007E-02
43.45	2.701E-01	3.4	45.27	2.530E-01	8.661E-03
43.95	2.484E-01	4.8	45.79	2.326E-01	1.117E-02
44.45	2.137E-01	4.6	46.31	2.004E-01	9.192E-03
44.95	1.794E-01	3.9	46.82	1.683E-01	6.616E-03
45.45	1.668E-01	3.3	47.34	1.566E-01	5.143E-03
46.45	1.510E-01	3.2	48.37	1.419E-01	4.590E-03
46.95	1.486E-01	3.2	48.89	1.397E-01	4.527E-03
47.45	1.488E-01	3.3	49.40	1.400E-01	4.568E-03
47.95	1.467E-01	3.4	49.92	1.381E-01	4.714E-03
48.45	1.372E-01	3.6	50.43	1.292E-01	4.594E-03
48.95	1.598E-01	3.1	50.95	1.506E-01	4.641E-03
49.45	1.317E-01	4.4	51.46	1.242E-01	5.497E-03
50.45	1.112E-01	4.8	52.49	1.050E-01	5.089E-03
51.95	7.308E-02	8.0	54.04	6.913E-02	5.518E-03
53.45	6.681E-02	4.9	55.58	6.332E-02	3.134E-03
54.95	6.322E-02	4.8	57.12	6.003E-02	2.901E-03
56.45	5.530E-02	4.8	58.66	5.262E-02	2.512E-03
57.95	4.555E-02	5.4	60.20	4.343E-02	2.332E-03
59.45	3.665E-02	6.6	61.73	3.501E-02	2.302E-03
60.95	4.127E-02	5.4	63.27	3.951E-02	2.136E-03
62.45	4.189E-02	5.5	64.80	4.019E-02	2.196E-03
63.95	3.737E-02	5.4	66.33	3.593E-02	1.958E-03
65.45	3.877E-02	6.2	67.86	3.736E-02	2.309E-03
66.95	3.126E-02	6.4	69.39	3.019E-02	1.937E-03
68.45	3.618E-02	5.4	70.91	3.501E-02	1.879E-03
69.95	2.904E-02	8.4	72.44	2.817E-02	2.361E-03
71.45	2.456E-02	8.7	73.96	2.388E-02	2.080E-03
72.95	2.715E-02	7.7	75.48	2.646E-02	2.047E-03

SCATTERING OF 104 MEV ALPHAPARTICLES CN 116 SN

Q = 0.0 MEV I = 0+

ECM = 100.532 MEV K = 4.3135/FERMI ETA = 3.08900

LABORATORY DATA THETA DEGREE	SIGMA MB/SR	DSIGMA %	RUTHERFORD SIGMA/SR	CM DATA THETA DEGREE	SIGMA MB/SR	DSIGMA MB/SR
7.55	3.010E+04	4.8	4.729E-01	7.82	2.809E+04	1.346E+03
8.05	2.290E+04	4.8	4.648E-01	8.33	2.137E+04	1.023E+03
8.55	1.915E+04	3.8	4.945E-01	8.85	1.788E+04	6.714E+02
9.05	1.572E+04	5.0	5.093E-01	9.37	1.468E+04	7.347E+02
9.55	1.129E+04	7.1	4.533E-01	9.89	1.054E+04	7.496E+02
10.05	7.696E+03	9.1	3.788E-01	10.40	7.186E+03	6.562E+02
10.55	4.273E+03	11.8	2.553E-01	10.92	3.990E+03	4.728E+02
11.05	2.638E+03	9.3	1.856E-01	11.44	2.464E+03	2.281E+02
11.55	1.837E+03	5.8	1.575E-01	11.96	1.716E+03	9.976E+01
12.05	1.577E+03	1.7	1.601E-01	12.47	1.473E+03	2.479E+01
12.55	1.589E+03	0.6	1.856E-01	12.99	1.485E+03	9.009E+00
13.05	1.581E+03	0.5	2.205E-01	13.51	1.477E+03	7.809E+00
13.55	1.540E+03	2.4	2.494E-01	14.03	1.439E+03	3.429E+01
14.05	1.228E+03	5.6	2.258E-01	14.54	1.148E+03	6.405E+01
14.55	8.612E+02	8.3	1.852E-01	15.06	8.051E+02	6.691E+01
15.05	5.140E+02	11.6	1.264E-01	15.58	4.806E+02	5.598E+01
15.55	2.650E+02	14.1	7.422E-02	16.09	2.478E+02	3.502E+01
16.05	1.416E+02	10.6	4.498E-02	16.61	1.324E+02	1.403E+01
16.55	1.163E+02	1.6	4.173E-02	17.13	1.088E+02	1.705E+00
17.05	1.557E+02	5.5	6.288E-02	17.65	1.457E+02	7.999E+00
17.55	2.013E+02	4.4	9.117E-02	18.16	1.884E+02	8.257E+00
18.05	2.436E+02	1.5	1.233E-01	18.68	2.280E+02	3.394E+00
18.55	2.330E+02	2.5	1.315E-01	19.20	2.181E+02	5.361E+00
19.05	1.876E+02	5.8	1.176E-01	19.71	1.757E+02	1.018E+01
19.55	1.246E+02	9.8	8.657E-02	20.23	1.167E+02	1.149E+01
20.05	6.552E+01	14.9	5.031E-02	20.75	6.137E+01	9.122E+00
20.55	2.736E+01	20.4	2.316E-02	21.26	2.563E+01	5.232E+00
21.05	9.756E+00	21.2	9.083E-03	21.78	9.142E+00	1.939E+00
21.55	6.751E+00	8.7	6.856E-03	22.30	6.328E+00	5.517E-01
22.05	1.555E+01	16.6	1.739E-02	22.81	1.458E+01	2.419E+00
22.55	3.251E+01	9.6	3.973E-02	23.33	3.049E+01	2.922E+00
23.05	4.655E+01	3.5	6.203E-02	23.84	4.366E+01	1.529E+00
23.55	4.858E+01	0.7	7.045E-02	24.36	4.558E+01	3.183E-01
24.05	4.461E+01	3.5	7.028E-02	24.88	4.186E+01	1.484E+00
24.55	3.318E+01	7.0	5.669E-02	25.39	3.114E+01	2.181E+00
25.05	2.148E+01	10.8	3.973E-02	25.91	2.017E+01	2.174E+00
25.55	1.010E+01	18.3	2.019E-02	26.43	9.485E+00	1.734E+00
26.05	3.051E+00	31.2	6.583E-03	26.94	2.866E+00	8.932E-01
26.55	6.020E-01	20.9	1.400E-03	27.46	5.657E-01	1.183E-01
27.05	1.801E+00	25.1	4.505E-03	27.97	1.693E+00	4.253E-01
27.55	5.104E+00	13.0	1.372E-02	28.49	4.799E+00	6.256E-01
28.05	8.426E+00	6.9	2.430E-02	29.00	7.924E+00	5.501E-01
28.55	1.093E+01	2.5	3.379E-02	29.52	1.028E+01	2.605E-01
29.05	1.100E+01	1.5	3.640E-02	30.04	1.035E+01	1.578E-01
29.55	9.485E+00	5.2	3.355E-02	30.55	8.928E+00	4.598E-01
30.05	6.140E+00	8.9	2.319E-02	31.07	5.781E+00	5.131E-01
30.55	4.060E+00	11.7	1.636E-02	31.58	3.824E+00	4.464E-01
31.05	1.430E+00	24.6	6.137E-03	32.10	1.347E+00	3.319E-01
31.55	5.467E-01	18.1	2.457E-03	32.61	5.152E-01	9.337E-02
32.05	4.543E-01	17.3	2.206E-03	33.13	4.283E-01	7.397E-02
32.55	1.307E+00	12.9	6.742E-03	33.64	1.233E+00	1.592E-01
33.55	2.936E+00	4.7	1.704E-02	34.67	2.771E+00	1.309E-01
34.05	3.434E+00	1.4	2.110E-02	35.19	3.242E+00	4.602E-02
34.55	3.202E+00	3.0	2.082E-02	35.70	3.024E+00	9.023E-02
35.05	2.563E+00	5.0	1.762E-02	36.22	2.421E+00	1.215E-01
35.55	1.964E+00	6.3	1.426E-02	36.73	1.856E+00	1.168E-01
36.05	1.366E+00	9.3	1.047E-02	37.24	1.291E+00	1.201E-01
36.55	7.218E-01	12.2	5.836E-03	37.76	6.826E-01	8.311E-02
37.05	5.094E-01	5.8	4.341E-03	38.27	4.819E-01	2.815E-02
37.55	4.751E-01	6.4	4.263E-03	38.79	4.496E-01	2.866E-02
38.05	7.667E-01	6.3	7.240E-03	39.30	7.258E-01	4.545E-02
38.55	9.130E-01	4.3	9.066E-03	39.81	8.647E-01	3.757E-02
39.05	1.101E+00	3.6	1.149E-02	40.33	1.043E+00	3.778E-02
39.55	1.237E+00	2.4	1.355E-02	40.84	1.172E+00	2.826E-02
40.05	1.271E+00	2.1	1.461E-02	41.36	1.205E+00	2.515E-02
40.55	1.144E+00	3.6	1.379E-02	41.87	1.085E+00	3.862E-02
41.05	9.470E-01	5.1	1.157E-02	42.38	8.986E-01	4.558E-02
41.55	7.195E-01	6.5	9.524E-03	42.90	6.830E-01	4.435E-02
42.05	5.227E-01	7.0	7.242E-03	43.41	4.964E-01	3.494E-02
42.55	3.897E-01	6.2	5.649E-03	43.92	3.702E-01	2.312E-02
43.05	3.249E-01	4.5	4.924E-03	44.44	3.088E-01	1.379E-02
43.55	3.305E-01	4.2	5.234E-03	44.95	3.143E-01	1.325E-02
44.05	3.780E-01	4.2	6.252E-03	45.46	3.596E-01	1.500E-02
44.55	4.077E-01	4.3	7.039E-03	45.97	3.880E-01	1.687E-02
45.05	4.816E-01	3.7	8.674E-03	46.49	4.585E-01	1.676E-02
45.55	4.791E-01	3.5	8.998E-03	47.00	4.563E-01	1.575E-02
46.05	4.441E-01	4.1	8.692E-03	47.51	4.232E-01	1.746E-02
46.55	3.812E-01	4.2	7.772E-03	48.02	3.634E-01	1.544E-02
47.05	3.617E-01	5.1	7.678E-03	48.54	3.450E-01	1.743E-02
47.55	2.579E-01	7.2	5.657E-03	49.05	2.461E-01	1.775E-02
48.05	2.150E-01	6.6	4.940E-03	49.56	2.052E-01	1.360E-02
48.55	1.518E-01	7.5	3.626E-03	50.07	1.450E-01	1.083E-02
49.05	1.351E-01	5.8	3.354E-03	50.58	1.291E-01	7.455E-03
49.55	1.369E-01	5.8	3.531E-03	51.09	1.309E-01	7.544E-03
50.05	1.363E-01	6.0	3.650E-03	51.61	1.304E-01	7.792E-03
50.55	1.166E-01	6.7	3.241E-03	52.12	1.116E-01	7.445E-03
51.05	1.213E-01	6.1	3.457E-03	52.63	1.161E-01	7.028E-03
51.55	1.215E-01	6.5	3.633E-03	53.14	1.164E-01	7.512E-03
52.05	9.075E-02	7.7	2.813E-03	53.65	8.696E-02	6.653E-03
52.55	9.349E-02	7.0	3.003E-03	54.16	8.963E-02	6.239E-03
53.55	7.152E-02	9.4	2.463E-03	55.18	6.863E-02	6.474E-03
54.05	5.241E-02	10.4	1.868E-03	55.69	5.032E-02	5.254E-03
55.05	4.661E-02	11.3	1.778E-03	56.71	4.479E-02	5.055E-03
55.55	3.113E-02	11.9	1.228E-03	57.22	2.993E-02	3.567E-03
56.55	3.951E-02	11.0	1.664E-03	58.24	3.803E-02	4.194E-03
58.05	2.885E-02	13.4	1.337E-03	59.77	2.781E-02	3.734E-03
59.55	2.351E-02	15.7	1.196E-03	61.30	2.270E-02	3.572E-03
61.05	1.056E-02	21.5	5.878E-04	62.83	1.021E-02	2.196E-03
62.55	1.449E-02	20.6	8.803E-04	64.35	1.404E-02	2.898E-03
64.05	1.722E-02	18.7	1.139E-03	65.87	1.671E-02	3.130E-03
65.55	8.378E-03	30.4	6.018E-04	67.40	8.142E-03	2.473E-03

SCATTERING OF 104 MEV ALPHAPARTICLES ON 116 ZR

Q = -1.293 MEV I = 2+

ECM = 99.239 MEV K = 4.2857/FERMI ETA = 3.10906

LABORATORY DATA			CM DATA		
THETA DEGREE	SIGMA MB/SR	DSIGMA %	THETA DEGREE	SIGMA MB/SR	DSIGMA MB/SR
7.55	1.967E+01	21.8	7.82	1.835E+01	4.002E+00
8.05	1.595E+01	27.9	8.34	1.488E+01	4.158E+00
8.55	3.753E+00	73.0	8.85	3.502E+00	2.558E+00
9.05	2.352E+01	16.0	9.37	2.195E+01	3.505E+00
9.55	3.297E+01	8.6	9.89	2.993E+01	2.584E+00
10.05	3.900E+01	6.2	10.41	3.640E+01	2.273E+00
10.55	4.404E+01	6.1	10.92	4.111E+01	2.511E+00
11.05	4.293E+01	6.2	11.44	4.008E+01	2.504E+00
11.55	3.905E+01	7.4	11.96	3.646E+01	2.686E+00
12.05	2.195E+01	15.4	12.48	2.050E+01	3.149E+00
12.55	8.250E+00	27.2	12.99	7.705E+00	2.092E+00
13.05	2.421E+00	44.8	13.51	2.261E+00	1.014E+00
13.55	2.987E-02	2971.7	14.03	2.790E-02	8.291E-01
14.05	4.581E+00	29.1	14.55	4.280E+00	1.245E+00
14.55	1.036E+01	10.9	15.06	9.681E+00	1.051E+00
15.05	1.330E+01	9.0	15.58	1.243E+01	1.123E+00
15.55	1.553E+01	7.8	16.10	1.452E+01	1.126E+00
16.05	1.863E+01	4.3	16.61	1.742E+01	7.433E-01
16.55	1.338E+01	8.3	17.13	1.251E+01	1.035E+00
17.05	8.405E+00	11.3	17.65	7.861E+00	8.870E-01
17.55	4.205E+00	17.4	18.17	3.933E+00	6.839E-01
18.05	1.208E+00	35.4	18.68	1.130E+00	4.002E-01
18.55	2.502E-01	32.7	19.20	2.341E-01	7.662E-02
19.05	1.287E+00	20.3	19.72	1.205E+00	2.451E-01
19.55	2.738E+00	17.3	20.23	2.563E+00	4.436E-01
20.05	5.519E+00	8.0	20.75	5.168E+00	4.117E-01
20.55	6.702E+00	2.8	21.27	6.277E+00	1.775E-01
21.05	6.739E+00	2.6	21.78	6.313E+00	1.646E-01
21.55	5.690E+00	4.5	22.30	5.331E+00	2.385E-01
22.05	4.377E+00	7.2	22.82	4.102E+00	2.959E-01
22.55	2.644E+00	13.8	23.33	2.478E+00	3.423E-01
23.05	8.587E-01	28.0	23.85	8.051E-01	2.251E-01
23.55	2.836E-01	21.4	24.37	2.660E-01	5.681E-02
24.05	3.601E-01	24.0	24.88	3.378E-01	8.114E-02
24.55	1.011E+00	14.2	25.40	9.486E-01	1.351E-01
25.05	1.728E+00	9.2	25.91	1.622E+00	1.488E-01
25.55	2.499E+00	5.4	26.43	2.346E+00	1.275E-01
26.05	2.986E+00	1.7	26.95	2.804E+00	4.872E-02
26.55	2.755E+00	2.3	27.46	2.588E+00	5.839E-02
27.05	2.443E+00	4.9	27.98	2.295E+00	1.121E-01
27.55	1.681E+00	9.2	28.49	1.580E+00	1.454E-01
28.05	9.368E-01	13.5	29.01	8.807E-01	1.193E-01
28.55	4.262E-01	17.5	29.53	4.008E-01	7.003E-02
29.05	2.307E-01	9.7	30.04	2.170E-01	2.104E-02
29.55	2.624E-01	15.2	30.56	2.469E-01	3.741E-02
30.05	6.104E-01	10.7	31.07	5.745E-01	6.161E-02
30.55	8.920E-01	7.4	31.59	8.398E-01	6.182E-02
31.05	1.215E+00	3.7	32.10	1.144E+00	4.281E-02
31.55	1.274E+00	2.0	32.62	1.200E+00	2.441E-02
32.05	1.250E+00	3.6	33.13	1.178E+00	4.211E-02
32.55	9.533E-01	6.0	33.65	8.987E-01	5.372E-02
33.55	5.012E-01	10.0	34.68	4.728E-01	4.742E-02
34.05	2.670E-01	12.7	35.19	2.520E-01	3.207E-02
34.55	1.858E-01	5.8	35.71	1.754E-01	1.009E-02
35.05	2.697E-01	6.7	36.22	2.547E-01	1.702E-02
35.55	3.165E-01	6.4	36.74	2.990E-01	1.908E-02
36.05	4.215E-01	6.2	37.25	3.983E-01	2.471E-02
36.55	5.275E-01	3.4	37.77	4.987E-01	1.689E-02
37.05	4.717E-01	3.5	38.28	4.461E-01	1.574E-02
37.55	4.938E-01	3.5	38.79	4.671E-01	1.658E-02
38.05	4.042E-01	8.3	39.31	3.825E-01	3.169E-02
38.55	1.919E-01	17.0	39.82	1.817E-01	3.092E-02
39.05	1.082E-01	14.2	40.34	1.025E-01	1.459E-02
39.55	8.877E-02	11.1	40.85	8.411E-02	9.365E-03
40.05	9.143E-02	10.2	41.36	8.666E-02	8.866E-03
40.55	1.167E-01	9.0	41.88	1.107E-01	9.921E-03
41.05	1.455E-01	8.0	42.39	1.380E-01	1.098E-02
41.55	1.778E-01	6.7	42.90	1.687E-01	1.131E-02
42.05	2.067E-01	5.8	43.42	1.962E-01	1.132E-02
42.55	2.290E-01	4.8	43.93	2.175E-01	1.049E-02
43.05	2.168E-01	5.3	44.44	2.060E-01	1.088E-02
43.55	1.947E-01	6.3	44.96	1.851E-01	1.171E-02
44.05	1.483E-01	7.9	45.47	1.410E-01	1.115E-02
44.55	1.242E-01	7.5	45.98	1.182E-01	8.809E-03
45.05	1.086E-01	7.8	46.50	1.034E-01	8.081E-03
45.55	9.369E-02	8.5	47.01	8.921E-02	7.542E-03
46.05	8.060E-02	8.5	47.52	7.678E-02	6.539E-03
46.55	9.034E-02	7.6	48.03	8.610E-02	6.573E-03
47.05	8.780E-02	8.2	48.54	8.372E-02	6.893E-03
47.55	9.952E-02	7.3	49.06	9.493E-02	6.954E-03
48.05	8.446E-02	7.4	49.57	8.060E-02	5.976E-03
48.55	8.742E-02	7.3	50.08	8.347E-02	6.086E-03
49.05	1.000E-01	6.7	50.59	9.556E-02	6.374E-03
49.55	8.933E-02	8.3	51.10	8.537E-02	7.053E-03
50.05	6.882E-02	9.1	51.62	6.580E-02	6.013E-03
50.55	6.821E-02	8.4	52.13	6.525E-02	5.486E-03
51.05	6.093E-02	9.2	52.64	5.831E-02	5.349E-03
51.55	4.556E-02	10.3	53.15	4.362E-02	4.500E-03
52.05	5.300E-02	9.2	53.66	5.077E-02	4.661E-03
52.55	3.367E-02	13.3	54.17	3.227E-02	4.288E-03
53.55	3.838E-02	12.2	55.19	3.682E-02	4.509E-03
54.05	3.951E-02	10.8	55.70	3.792E-02	4.110E-03
55.05	4.081E-02	12.2	56.72	3.921E-02	4.777E-03
55.55	3.281E-02	12.2	57.23	3.154E-02	3.840E-03
56.55	2.670E-02	14.0	58.25	2.569E-02	3.606E-03
58.05	2.211E-02	14.9	59.78	2.131E-02	3.185E-03
59.55	1.992E-02	16.8	61.31	1.923E-02	3.224E-03
61.05	5.992E-03	44.7	62.84	5.793E-03	2.588E-03
62.55	1.580E-02	19.5	64.36	1.530E-02	2.977E-03
64.05	1.115E-02	24.3	65.89	1.082E-02	2.628E-03
65.55	5.777E-03	34.0	67.41	5.613E-03	1.910E-03

SCATTERING OF 104 MEV ALPHAPARTICLES ON 116 SN

Q = -2.266 MEV I = 3-

ECM = 98.266 MEV K = 4.2646/FERMI ETA = 3.12441

LABORATORY DATA			CM DATA		
THETA DEGREE	SIGMA MB/SR	DSIGMA %	THETA DEGREE	SIGMA MB/SR	DSIGMA MB/SR
8.55	2.980E+01	9.6	8.86	2.780E+01	2.65E+00
9.05	2.612E+01	14.0	9.37	2.437E+01	3.41E+00
9.55	6.802E+00	41.0	9.89	6.346E+00	2.60E+00
10.05	8.081E+00	19.2	10.41	7.54CE+00	1.44E+00
10.55	2.286E+00	64.7	10.93	2.133E+00	1.38CE+00
11.05	5.451E+00	33.6	11.44	5.087E+00	1.70E+00
11.55	1.262E+01	16.5	11.96	1.17EE+01	1.94E+00
12.05	2.121E+01	7.8	12.48	1.98CE+01	1.53E+00
12.55	2.247E+01	6.1	13.00	2.09EE+01	1.28E+00
13.05	2.382E+01	4.2	13.51	2.224E+01	9.29E-01
13.55	2.269E+01	7.2	14.03	2.11EE+01	1.53E+00
14.05	1.481E+01	12.4	14.55	1.383E+01	1.72E+00
14.55	8.274E+00	15.4	15.07	7.72EE+00	1.18E+00
15.05	3.797E+00	28.6	15.58	3.54EE+00	1.01E+00
15.55	1.647E-0343398.3		16.10	1.53EE-03	6.67E-01
16.05	2.C75E+00	36.8	16.62	1.93EE+00	7.14CE-01
16.55	6.194E+00	12.8	17.13	5.79CE+00	7.38E-01
17.05	9.246E+00	5.9	17.65	8.644E+00	5.10E-01
17.55	1.103E+01	3.8	18.17	1.031E+01	3.91E-01
18.05	1.295E+01	4.0	18.69	1.211E+01	4.80E-01
18.55	8.131E+00	7.8	19.20	7.60EE+00	5.90E-01
19.05	7.318E+00	6.1	19.72	6.847E+00	4.15E-01
19.55	4.052E+00	15.3	20.24	3.792E+00	5.79E-01
20.05	1.784E+00	19.4	20.75	1.67CE+00	3.23E-01
20.55	8.948E-01	13.2	21.27	8.377E-01	1.10E-01
21.05	8.959E-01	10.5	21.79	8.39CE-01	8.81E-02
21.55	1.515E+00	13.0	22.30	1.41EE+00	1.84E-01
22.05	2.782E+00	10.3	22.82	2.60EE+00	2.69E-01
22.55	4.303E+00	6.1	23.34	4.032E+00	2.45E-01
23.05	5.099E+00	1.9	23.85	4.77EE+00	9.18E-02
23.55	4.591E+00	3.5	24.37	4.304E+00	1.49E-01
24.05	3.788E+00	5.7	24.85	3.552E+00	2.01CE-01
24.55	2.764E+00	8.2	25.40	2.593E+00	2.11E-01
25.05	1.640E+00	12.7	25.92	1.53EE+00	1.95E-01
25.55	7.619E-01	16.0	26.43	7.15OE-01	1.14E-01
26.05	4.741E-01	6.8	26.95	4.451E-01	3.02EE-02
26.55	5.430E-01	10.6	27.47	5.09EE-01	5.42E-02
27.05	1.026E+00	11.2	27.98	9.641E-01	1.07E-01
27.55	1.027E+00	5.9	28.50	1.52EE+00	8.99E-02
28.05	1.912E+00	2.9	29.01	1.797E+00	5.18E-02
28.55	2.107E+00	2.3	29.53	1.98IE+00	4.59E-02
29.05	2.036E+00	3.0	30.05	1.91EE+00	5.80E-02
29.55	1.623E+00	6.2	30.56	1.52EE+00	9.50E-02
30.05	1.056E+00	8.3	31.08	9.932E-01	8.28E-02
30.55	7.772E-01	8.5	31.59	7.31EE-01	6.21E-02
31.05	4.504E-01	11.1	32.11	4.241E-01	4.69E-02
31.55	3.117E-01	5.4	32.62	2.936E-01	1.58E-02
32.05	3.880E-01	8.1	33.14	3.655E-01	2.97EE-02
32.55	5.580E-01	6.6	33.65	5.259E-01	3.49EE-02
33.55	8.578E-01	4.1	34.68	8.09CE-01	3.29E-02
34.05	9.378E-01	2.4	35.20	8.847E-01	2.14E-02
34.55	8.070E-01	4.6	35.71	7.61EE-01	3.53EE-02
35.05	6.266E-01	5.6	36.23	5.91EE-01	3.31EE-02
35.55	5.102E-01	5.7	36.74	4.818E-01	2.76IE-02
36.05	3.896E-01	7.7	37.26	3.681E-01	2.84IE-02
36.55	2.595E-01	8.3	37.77	2.452E-01	2.03EE-02
37.05	2.241E-01	5.7	38.29	2.11EE-01	1.21EE-02
37.55	2.315E-01	5.9	38.80	2.18EE-01	1.29EE-02
38.05	2.472E-01	5.3	39.31	2.33EE-01	1.25IE-02
38.55	2.633E-01	5.7	39.83	2.492E-01	1.42IE-02
39.05	2.981E-01	4.8	40.34	2.823E-01	1.35EE-02
39.55	3.203E-01	4.2	40.86	3.034E-01	1.27EE-02
40.05	3.058E-01	4.4	41.37	2.89EE-01	1.27EE-02
40.55	3.005E-01	4.7	41.88	2.84EE-01	1.35IE-02
41.05	2.625E-01	6.0	42.40	2.48EE-01	1.48EE-02
41.55	2.105E-01	7.8	42.91	1.997E-01	1.54EE-02
42.05	1.495E-01	8.4	43.42	1.41EE-01	1.19EE-02
42.55	1.435E-01	8.5	43.94	1.36IE-01	1.15EE-02
43.05	7.704E-02	11.8	44.45	7.31EE-02	8.64EE-03
43.55	1.235E-01	8.7	44.96	1.174E-01	1.02EE-02
44.05	1.343E-01	7.2	45.48	1.277E-01	9.13E-03
44.55	1.528E-01	6.4	45.99	1.453E-01	9.29EE-03
45.05	1.554E-01	6.5	46.50	1.47EE-01	9.61EE-03
45.55	1.595E-01	6.2	47.01	1.51EE-01	9.39EE-03
46.05	1.598E-01	6.9	47.53	1.522E-01	1.04EE-02
46.55	1.148E-01	9.8	48.04	1.09EE-01	1.07EE-02
47.05	8.825E-02	10.9	48.55	8.413E-02	9.14E-03
47.55	6.623E-02	12.0	49.06	6.31EE-02	7.56OE-03
48.05	7.605E-02	8.6	49.58	7.25EE-02	6.21EE-03
48.55	7.790E-02	8.4	50.09	7.43EE-02	6.24EE-03
49.05	6.973E-02	9.1	50.60	6.65EE-02	6.08EE-03
49.55	5.840E-02	10.5	51.11	5.58OE-02	5.87OE-03
50.05	7.405E-02	8.7	51.62	7.07EE-02	6.17EE-03
50.55	7.779E-02	7.8	52.13	7.44OE-02	5.81EE-03
51.05	6.980E-02	9.1	52.65	6.67EE-02	6.10EE-03
51.55	6.151E-02	11.0	53.16	5.88EE-02	6.45EE-03
52.05	5.443E-02	11.1	53.67	5.21EE-02	5.77EE-03
52.55	4.587E-02	12.4	54.18	4.39EE-02	5.44EE-03
53.55	4.248E-02	14.2	55.20	4.07EE-02	5.79EE-03
54.05	2.131E-02	24.9	55.71	2.045E-02	5.08EE-03
55.05	3.653E-02	13.7	56.73	3.50EE-02	4.82OE-03
55.55	3.317E-02	11.6	57.24	3.18EE-02	3.71EE-03
56.55	3.675E-02	13.8	58.26	3.53EE-02	4.89OE-03
58.05	3.077E-02	14.1	59.79	2.96EE-02	4.18EE-03
59.55	1.073E-02	30.0	61.32	1.036E-02	3.10E-03
61.05	3.102E-03	77.5	62.84	2.99EE-03	2.32EE-03
62.55	6.647E-03	34.1	64.37	6.43EE-03	2.19EE-03
64.05	1.506E-02	19.3	65.89	1.461E-02	2.82EE-03
65.55	3.789E-03	51.2	67.42	3.68IE-03	1.88EE-03